ADDIS ABABA UNIVERSITY

ADDIS ABABA INSTITUTE OF TECHNOLOGY

SCHOOL OF CIVIL AND ENVIRONMENTAL ENGINEERING

Linear and Geometric Nonlinear Effect of Axial Load on Flexural Deformation of Reinforced Concrete Members

---

A Thesis in Structural Engineering

By Bayelign Hailegiorgis

April, 2018

Addis Ababa

A Thesis

Submitted in Partial Fulfillment of the Requirements for the Degree of Master of Science in Civil Engineering

The undersigned have examined the thesis entitled '**Linear and Geometric Nonlinear Effect of Axial Load on Flexural Deformation of Reinforced Concrete Members**' presented by **Bayelign Hailegiorgis**, a candidate for the degree of **Master of Science** and hereby certify that it is worthy of acceptance.

Abrham Gebre (PhD)	_____	_____
Advisor	Signature	Date
Asnake Adamu (PhD)	_____	_____
Internal Examiner	Signature	Date
Girma Zerayohnnes (PhD)	_____	_____
External Examiner	Signature	Date
Agizew Nigussie (PhD)	_____	_____
Chairperson	Signature	Date

UNDERTAKING

I certify that research work titled “Linear and Geometric Nonlinear Effect of Axial Load on Flexural deformation of Reinforced Concrete Members” is my own work. The work has not been presented elsewhere for assessment. Where material has been used from other sources it has been properly acknowledged / referred.

Bayelign Hailegiorgis

ACKNOWLEDGMENTS

First of all, I would like to thank to my MSc advisor, Abrham Gebre (Ph.D), for supporting me during my thesis work and sharing his great knowledge and experience with me. Without his supervision and constant help, this Thesis would not have been possible. Under his guidance I successfully overcame many difficulties and learned a lot. It has been an honor to be his student.

I am also thankful to Mr. Andargachew, Solomon, Garomisa and Tina for their helping and Advise to complete the final goal of my thesis, you were my strength when I was doing my thesis.

Last but certainly not least, I would like to thank my family members and friends for their invaluable support.

ABSTRACT

The problem of a concrete cross section under flexural and axial loading is indeterminate due to the existence of more unknowns than equations. Therefore proper analysis of reinforced concrete member is important for understanding the actual behavior and economical use of sections. The main objective of this Thesis is to investigate geometric nonlinear effect of axial load on flexural deformation of reinforced concrete members. Flexural members, which are subjected to gravity central point load, external compressive axial load and combination of those load with different support conditions, cross section and span length are analysed using linear and geometric nonlinear method of analysis to investigate the effect of axial load on flexural deformation of flexural members. The percentage variation of flexural deformation under linear and geometric nonlinear analysis for various conditions of members is calculated to achieve the objective. Finally four story reinforced concrete residential building frame is analysed using linear and geometric nonlinear analysis. Both linear and geometric nonlinear analysis is done by using STAAD Pro and linear analysis using FEM based code using Scilab and ETABS. After the analysis of flexural members it is found that: The percentage variation of linear and geometrical nonlinear deflection is very high for beam with lesser depth. It was found that the support conditions also affect variation of deflection for the linear and nonlinear cases. The variation between linear and geometrical nonlinear deflection of beam is negligible when the ends are fixed. But for the same beam with simply supported end conditions the defections were found having variation up to 17.571 percentages. Geometrical nonlinearity is more when the load is very high and lesser depth. At the initial stages of loading behavior of beam is linear only and it behaves nonlinear when we go for higher loads. As the deforming of middle plane (Neutral axis) starts, the stiffness of structure increases (axial stiffness is added with bending stiffness).Thus the beam becomes stiffer progressively. It is a positive aspect of geometric nonlinearity.

Keywords: - Nonlinear Analysis, Finite Element Method, Flexural Deformation, Reinforced Concrete Beam, STAAD.Pro, Scilab.code

TABLE OF CONTENTS

LIST OF TABLES

LIST OF FIGURES

LIST OF SYMBOLS

A cross sectional area

{a} vector coefficients in assumed displacement field

[B] element strain displacement matrix

d nodal displacement

E modulus of elasticity

F force

f_b bending stress

G shear modulus

I moment of inertia of cross sectional area

[K] global stiffness matrix

$[k_e]$ elastic stiffness matrix

$[k_g]$ geometric stiffness matrix

L length

[L] linear differential operator relating the rotation, transformation matrix

M bending moment

N shape function or blending function

[N] element shape function matrix

p axial load

P_{cr} buckling load

[p] polynomial series coefficient matrix

U displacement

u nodal displacement

U strain energy

U^e element strain energy

W work

φ field variable

θ nodal rotation

ε strain

Δ displacement

ρ mass density or radius of curvature

Π potential energy

Π^e element potential energy

σ stress

1. Introduction

1.1 Background

Reinforced concrete beams may also be subjected to axial forces, acting simultaneously with shear and flexure, due to a variety of causes. These include external axial loads, longitudinal prestressing and restrains forces introduced as a result of shrinkage of the concrete or temperature changes. Beams may have their strength in shear significantly modified in presence of axial tension or compression [1]. It is important to study the real behavior of the reinforced concrete beam loaded at the ends and the mid-span. For simplicity the linear nature of both material and geometry of structures are considered. In this assumption displacements and rotations are small, supports do not settle, stress is directly proportional to strain and loads maintain their original direction as the structure deforms. Equilibrium equation (Eq. 1.1) are written for original support condition, elastic stress-strain relation, load-force configuration and load directions.

$$F = K * U \tag{1.1}$$

in which [K] = a linear-elastic stiffness matrix

U = Displacement

F= force

$$U = K^{-1} * F \tag{1.2}$$

Displacement Eq. 1.2 are obtained in a single step of equation solving. Fortunate that so many practical problems can be solved by so simple an approximation. However, any of the convenient assumptions that leads to a linear analysis may be at odds with reality. Adjacent parts may make or break contact. A contact area may change as load changes. Elastic material may be come plastic, or the material may not have a linear stress- strain relation at any stress level. Part of the structure may lose stiffness because of buckling or failure of the material. Displacement and rotations may be come large enough that equilibrium equation must be written for the deformed configuration rather than the

original configuration. Thus, a geometric nonlinear analysis is carried out when a structure undergoes large displacements and the change of its geometric shape causes a nonlinear displacement-strain relationship. To address such concern geometric nonlinear method of analysis must be employed. Thus, there is a growing need for analysis method to study the real behavior of reinforced concrete members subjected to axial load.

1.2 Objective

The objective of this thesis is to investigate linear and geometric nonlinear effect of axial load on flexural deformation of reinforced concrete members.

1.3 Scope of the research

This thesis focuses on flexural deformation of reinforced concrete flexural members. This to emphasize on the role of axial load on flexural deformation for Reinforced concrete members. Such approach was used as it will show the objective of the thesis clearly.

1.4 Thesis organization

This thesis organized in five Chapters. Reasons for investigation and main objective are discussed in the first Chapter. The second Chapter presents literature review on axial load effect on flexural deformation. Furthermore the different source of nonlinearity, specifically geometric nonlinear analysis, are reviewed. Additionally theoretical background of linear and geometric nonlinear analysis is presented. This is accomplished by taking a representative flexural finite element members with six degree of freedom. The finite element member with six degree of freedom is used to derive elastic stiffness matrix and later geometric stiffness matrix is derived by considering the effect of axial load. Furthermore the different levels of analysis are presented and finally the combined effect of axial load and bending moment has been discussed

The third Chapter presents types of models that are going to be used in the analysis and finally the analysis of those modes have been done.

The fourth chapter presents the finding of analysis and discussion of the result. Three nodded beam with different support conditions, span length and thickness are analysed using software. Linear behavior is carried out using STAAD Pro and by finite element based scilab code. Nonlinear behavior is carried out using STAAD Pro. The effect of beam depth, length and support conditions on linear and geometric nonlinear problems are investigated. Furthermore four story reinforced concrete residential building is considered. The building first subjected to only earthquake (EQ) load and the corresponding lateral load at each story levels are calculated by using equivalent static analysis. Later the building is loaded both gravity load and earthquake load and the corresponding load in beams at each story has been transferred by using coefficient method. Then the representative frame is selected and linear and geometric nonlinear analysis is done to investigate the effect of axial load on flexural deformation of beam at a given story. The fifth Chapter presents the conclusion of the results made in chapter four. Recommendations are expressed at the end of the Chapter.

2. Literature Review

Structural analyses can be divided into two categories: linear and nonlinear. Nonlinear analyses consider the nonlinear system response. Nonlinear analyses are more difficult to perform than linear analyses however, they are more widely applicable. Many systems can be satisfactorily analyzed while assuming that the response of the system is linear under small loads and /or applied fields. However, nonlinear analysis techniques are required when analyses employing the linear assumption cannot satisfactorily describe the response of the system to large loads and/or applied fields.

Typical geometric nonlinearity arises from mid plane stretching of a thin structure coupled with transverse vibrations or loading. This stretching leads to a nonlinear relationship between the strain and the displacement. The non-linear analysis of beam is due to the bending of beam, and due to thin thickness of beam the neutral axis of beam is stretched due to this additional axial force is induced in the beam [2].

2.1 Linear Analysis

Linear analysis (first order analysis) is also known as linear elastic analysis. The term of Elastic means that when the structure is unloaded it follows the same deformation path as when loaded. In linear elastic analysis, the material is assumed to be unyielding and its properties invariable and the equations of equilibrium are formulated on the geometry of the unloaded structure. It is assumed that the subsequent deflections will be small and will have insignificant effect on the stability and mode of response of the structure [2].

In linear Finite element analysis, response is directly proportional to load. Linearity may be a good representation of reality or may only be the inevitable result of assumptions made for analysis purposes. In linear analysis we assume that displacements and rotations are small, supports do not settle, stress is directly proportional to strain and loads maintain their original direction as the structure deforms. Equilibrium equation Eq.1.1are written for original support condition, elastic stress-strain relation, load-force configuration and load directions. Displacement Eq.1.2 are obtained in a single step of equation solving.

Linear analysis in which structure which returns into original form after the removal of loads and there will be small changes in shape stiffness and no change in loading direction or magnitude. A linear FEA analysis is undertaken when a structure is expected to behave linearly, i.e. obeys Hook's Law. In linear elastic analysis, the material is assumed to be unyielding and its properties consistent and the equations of equilibrium are formulated on the geometry of the unloaded structure [3]. In this approach the primary unknowns are the joint displacements, which are determined first by solving the structure equation of equilibrium. Then, the unknown forces can be obtained through compatibility consideration. In geometrically linear analysis, the equations of equilibrium are formulated in the un-deformed state and are not updated with the deformation. This is valid in case of small deformation only.

2.1.1 Shape functions

The values of the field variable computed at the nodes are used to approximate the values at non nodal points (that is, in the element interior) by interpolation of the nodal values. For the three-node triangle example, the field variable is described by the approximate relation

$$\varphi(x,y) = N_1(x,y)\varphi_1 + N_2(x,y)\varphi_2 + N_3(x,y)\varphi_3 \qquad 2.1$$

where φ_1, φ_2, and φ_3 are the values of the field variable at the nodes, and N_1, N_2, and N_3 are the interpolation functions, also known as shape functions or blending functions. In the finite element approach, the nodal values of the field variable are treated as unknown constants that are to be determined. The interpolation functions are most often polynomial forms of the independent variables, derived to satisfy certain required conditions at the nodes.

The interpolation functions are predetermined, known functions of the independent variables; and these functions describe the variation of the field variable within the finite element.

Axial member

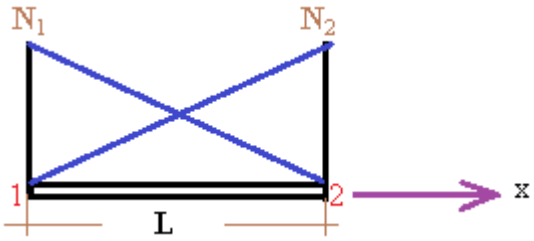

Figure 2.1 Axial Finite Element

With reference to Fig.2.1 one can start with

$$u = N_1 \bar{u}_1 + N_2 \bar{u}_2 \tag{2.2}$$

$$\theta_x = N_1 \theta_{x1} + N_2 \theta_{x2} \tag{2.3}$$

Since there are two degree of freedom, it can be assumed a linear deformation state

$$u = a_1 x + a_2 \tag{2.4}$$

Where u can be either u or θ and the boundary conditions are given by $u = \bar{u}_1$ at x=0 and $u = \bar{u}_2$ at x=L. Thus we have:

$$\bar{u}_1 = a_2 \tag{2.5}$$

$$\bar{u}_2 = a_1 L + a_2 \tag{2.6}$$

Solving for a_1 and a_2 in terms of $\bar{u}_1$ and $\bar{u}_2$ then obtain:

$$a_1 = \frac{\bar{u}_2}{L} - \frac{\bar{u}_1}{L} \tag{2.7}$$

$$a_2 = \bar{u}_1 \tag{2.8}$$

Substituting and rearranging those expression in to Eq. 2.4 obtain:

$$u = \left(\frac{\bar{u}_2}{L} - \frac{\bar{u}_1}{L} \right) x + \bar{u}_1 \tag{2.9}$$

$$u = \underbrace{(1 - \frac{x}{2})}_{N1} \bar{u}_1 + \underbrace{(\frac{x}{L})}_{N2} \bar{u}_2$$

Or:

$$N_1 = 1 - \frac{x}{L} \tag{2.10}$$

$$N_2 = \frac{x}{L}$$

Flexural Member

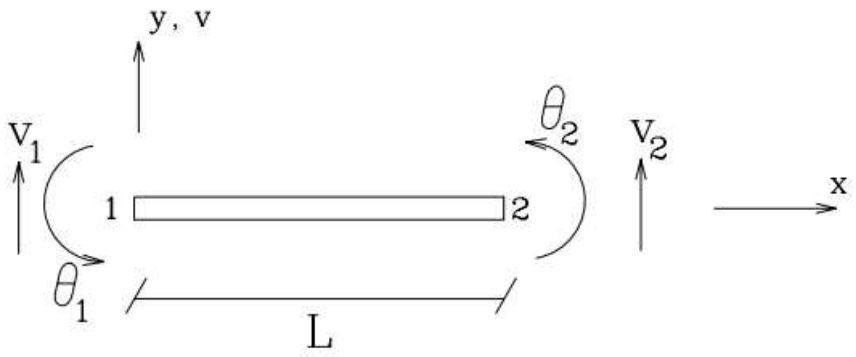

Figure 2.2 Flexural finite element [4]

With reference to Fig.2.2 one have four degree of freedoms $\{u\}_{4x1}$: and hence will need four shape functions, N_1 to N_4 and those can be obtained through four boundary conditions. Therefore it is needed to assume a polynomial approximation for displacements of degree 3.

$$v = a_1 x^3 + a_2 x^2 + a_3 x + a_4 \tag{2.11}$$

$$\theta = \frac{dv}{dx} = 3a_1 x^2 + 2a_2 x + a_3 \tag{2.12}$$

Note that v can be rewritten as:

$$v = \underbrace{\begin{bmatrix} x^3 & x^2 & x & 1 \end{bmatrix}}_{[P]} \underbrace{\begin{Bmatrix} a_1 \\ a_2 \\ a_3 \\ a_4 \end{Bmatrix}}_{\{u\}} \tag{2.13}$$

now apply the boundary conditions:

1. $v = \overline{v_1}$ at x=0
2. $v = \overline{v_2}$ at x=L

3. $\theta = \overline{\theta_1} = \dfrac{dv}{dx}$ at x=0

4. $\theta = \overline{\theta_2} = \dfrac{dv}{dx}$ at x=L

Or:

$$\underbrace{\begin{Bmatrix}\overline{v_1}\\ \overline{\theta_1}\\ \overline{v_2}\\ \overline{\theta_2}\end{Bmatrix}}_{\{\bar{u}\}} = \underbrace{\begin{bmatrix}0 & 0 & 0 & 1\\ 0 & 0 & 1 & 0\\ L^3 & L^2 & 1 & 1\\ 3L^2 & 2L & 1 & 0\end{bmatrix}}_{[L]} \underbrace{\begin{bmatrix}a_1\\ a_2\\ a_3\\ a_4\end{bmatrix}}_{\{a\}} \tag{2.14}$$

Table 2-1Characteristics of Beam Element Shape Functions

Function	$\xi = 0$		$\xi = 1$	
	N_i	$N_{i,x}$	N_i	$N_{i,x}$
$N1 = (1 + 2\xi^3 - 3\xi^2)$	1	0	0	0
$N2 = x(1 - \xi)^2$	0	1	0	0
$N3 = (3\xi^2 - 2\xi^3)$	0	0	1	0
$N4 = x(\xi^2 - \xi)$	0	0	0	1

When Eq.2.14 is inverted, it yields:

$$\underbrace{\begin{bmatrix}a_1\\ a_2\\ a_3\\ a_4\end{bmatrix}}_{\{a\}} = \frac{1}{L^3}\underbrace{\begin{bmatrix}2 & L & -2 & L\\ -3L & -2L^2 & 3L & -L^2\\ 0 & L^3 & 0 & 0\\ L^3 & 0 & 0 & 0\end{bmatrix}}_{[L]^{-1}} \underbrace{\begin{Bmatrix}\overline{v_1}\\ \overline{\theta_1}\\ \overline{v_2}\\ \overline{\theta_2}\end{Bmatrix}}_{\{\bar{u}\}} \tag{2.15}$$

Combining Eq. 2.15 with Eq. 2.13 to obtain:

$$u = \underbrace{\begin{bmatrix}x^3 & x^2 & x & 1\end{bmatrix}}_{[P]}\frac{1}{L^3}\underbrace{\begin{bmatrix}2 & L & -2 & L\\ -3L & -2L^2 & 3L & -L^2\\ 0 & L^3 & 0 & 0\\ L^3 & 0 & 0 & 0\end{bmatrix}}_{[L]^{-1}} \underbrace{\begin{Bmatrix}\overline{v_1}\\ \overline{\theta_1}\\ \overline{v_2}\\ \overline{\theta_2}\end{Bmatrix}}_{\{\bar{u}\}} \tag{2.16a}$$

$$u = \underbrace{\left[\underbrace{\left(1+2\xi^3-3\xi^2\right)}_{N_1} \quad \underbrace{x(1-\xi)2}_{N_2} \quad \underbrace{\left(3\xi 2-2\xi 3\right)}_{N_3} \quad \underbrace{\left(\xi 2-\xi\right)}_{N_4}\right]}_{\underbrace{[P][L]^{-1}}_{N}} \underbrace{\begin{Bmatrix} v_1 \\ \theta_1 \\ v_2 \\ \theta_2 \end{Bmatrix}}_{\{u\}} \tag{2.16b}$$

Where $\xi = \dfrac{x}{l}$

Hence the shape functions for the flexural element are given by:

$$N_1 = \left(1+\xi^3-3\xi^2\right) \tag{2.17a}$$

$$N_2 = x\left(1-\xi\ \right)^2 \tag{2.17b}$$

$$N_3 = \left(3\xi^2-\xi^3\right) \tag{2.17c}$$

$$N_4 = \left(\xi^2-\xi\right) \tag{2.17d}$$

The shape functions were obtained in earlier approach is based on lagrangian interpolation function and by:

1. Assumption of a polynomial function: u = [p]{a}
2. Application of the boundary conditions {u} = [*L*]{a}
3. Inversion of [*L*]
4. And finally [N] = [p][*L*]$^{-1}$

2.1.2 Finite Strain – Displacement Relation

The displacement Δ at any point inside an element can be written in terms of the shape functions N and the nodal displacements {Δ}

$$\Delta = [N]\{\Delta\} \tag{2.18}$$

The strain is then defined as:

$$\varepsilon = [B]\{\Delta\} \tag{2.19}$$

Where [B] is the matrix which relates joint displacement to strain fields

Axial Member

Using the shape function for axial member previously derived in Eq.2.10 one have:

$$u = \underbrace{\begin{bmatrix} \left(1-\frac{x}{L}\right) & \frac{x}{L} \end{bmatrix}}_{[N]} \underbrace{\begin{Bmatrix} u_1 \\ u_2 \end{Bmatrix}}_{\{\Delta\}} \tag{2.20a}$$

$$\varepsilon = \varepsilon_x = \underbrace{\begin{bmatrix} \underbrace{\frac{-1}{L}}_{\frac{\partial N_1}{\partial x}} & \underbrace{\frac{1}{L}}_{\frac{\partial N_2}{\partial x}} \end{bmatrix}}_{[B]} \underbrace{\begin{Bmatrix} u_1 \\ u_2 \end{Bmatrix}}_{\{\Delta\}} \tag{2.20b}$$

Flexural Member

Using the shape function for axial member previously derived in Eq.2.17 to have:

$$\varepsilon = \frac{y}{\rho} = y\frac{d^2v}{dx^2} \tag{2.21a}$$

$$\frac{1}{\rho} = \frac{M}{EI} \tag{2.21b}$$

$$\frac{1}{\rho} = y\frac{d^2v}{dx^2} \tag{2.21c}$$

$$\frac{1}{\rho} = y\underbrace{\begin{bmatrix} \underbrace{\frac{6}{L^2}(2\xi-1)}_{\frac{\partial^2 N_1}{\partial x^2}} & \underbrace{-\frac{2}{L}(3\xi-2)}_{\frac{\partial^2 N_2}{\partial x^2}} & \underbrace{\frac{6}{L^2}(-2\xi+1)}_{\frac{\partial^2 N_3}{\partial x^2}} & \underbrace{\frac{-2}{L}(3\xi-1)}_{\frac{\partial^2 N_4}{\partial x^2}} \end{bmatrix}}_{[B]} \underbrace{\begin{Bmatrix} v_1 \\ \theta_1 \\ v_2 \\ \theta_2 \end{Bmatrix}}_{\{\Delta\}} \tag{2.21d}$$

2.1.3 Linear Elastic Stiffness matrix

The beam element will be assumed to be a straight bar of uniform cross section capable of resisting axial forces, bending moments about the two principal axes in the plane of its

cross section, and twisting moments about its centroid axis. The following forces are acting on the beam in two-dimensional problems: axial forces S_1 and S_4; shearing forces $S_2$and S_5; bending moments $S_3$and S_6. The location and positive direction of these forces are shown in Fig. 2.3. The corresponding displacements u..... u_6 will be taken, as before, to be positive in the positive directions of the forces.

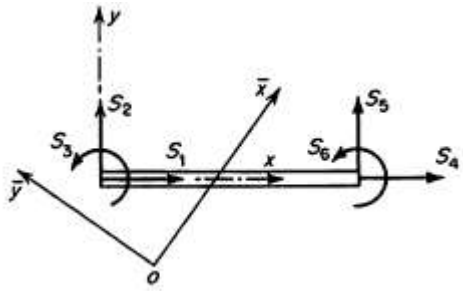

Figure 2.3 Beam element for two-dimensional structures [5]

In order to demonstrate the third method for obtaining force-displacement relationships, the stiffness properties for a uniform beam element will be derived directly from the differential equations for beam displacements used in the engineering beam theory. The stiffness coefficients derived from these equations will be exact within the limits of the assumptions in the general engineering theory of beams subjected to loads.

Axial Forces (S_1 and S_4)

The differential equation for the axial displacement u of the uniform beam shown in Fig. 2.4a is

$$S_1 = -\left(\frac{du}{dx}\right)EA \tag{2.22}$$

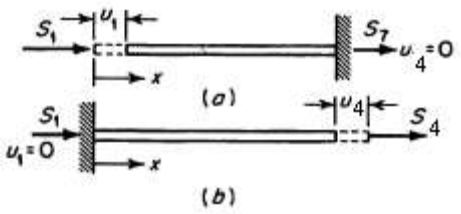

Figure 2.4 Axial Forces S_1 &S_4

Equation (2.22) can be integrated directly, so that

$$S_1 x = -uEA + C_1 \tag{2.23}$$

Where C_1 is a constant of integration. We shall assume that the left end of the beam at x = 0 has displacement u, while the displacement is zero at x = L. Hence

$$C_1 = S_1 L \tag{2.24}$$

Using Eqs. (2.23) and (2.24), for x = 0 we get

$$S_1 = \frac{EA}{L} u_1 \tag{2.25}$$

Also from the equation of equilibrium in the x direction it follows that

$$S_1 = -S_4 \tag{2.26}$$

Algebraic interpretation of the force-displacement relation $S = ku$ can be used to define individual stiffness coefficients k_{ij}. For example, k_{ii} represents the element force S_i due to unit displacement u_j when all other displacements are equal to zero.

$$k_{11} = \frac{EA}{L} \tag{2.27}$$

$$k_{41} = -\frac{EA}{L} \tag{2.28}$$

While all other coefficients in the first column of k are equal to zero.

Similarly, if $u_1 = 0$ and we allow u_4 to be nonzero (see Fig.2.4b), it can be shown, either from symmetry or from the solution for u that

$$k_{44} = \frac{EA}{L} \tag{2.29}$$

$$k_{14} = -\frac{EA}{L} \tag{2.30}$$

Shearing Forces (S_2 and S_5)

The lateral deflection v on the beam subjected to shearing forces and associated moments, as shown in Fig. 2.5a, is given by

$$v = v_b + v_s \tag{2.31}$$

Where v_b is the lateral deflection due to bending strains and v_s is the additional deflection due to shearing strains, such that

$$\frac{dv_s}{dx} = \frac{-S_2}{GA_s} \tag{2.32}$$

With A, representing the beam cross-sectional area effective in shear. The bending deflection for the beam shown in Fig. 2.5a is governed by the differential equation

$$EI \frac{d^2 v_b}{dx^2} = S_2 x - S_5 \tag{2.33}$$

From integration of Eqs. (2.32) and (2.33) it follows that

$$EIv = \frac{S_2 x^3}{6} - \frac{S_3 x^2}{2} + \left(C1 - \frac{S^2 EI}{GA_s} \right) x + C_2 \tag{2.34}$$

Where C, and C_2 are the constants of integration. Using the boundary conditions in Fig. 2.5a,

$$\frac{dv}{dx} = \frac{dv_s}{dx} = \frac{S_2}{GA_s} \qquad \text{at x= 0, x =L} \tag{2.35}$$

$$v = 0 \qquad \text{at x =L} \tag{2.36}$$

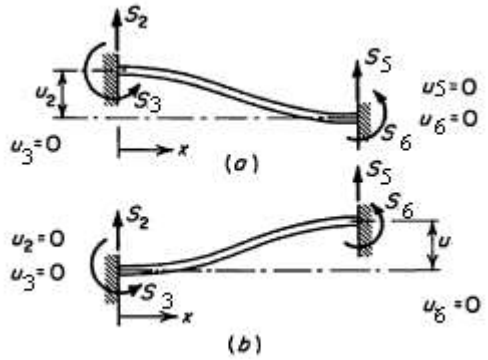

Figure 2.5 Shear forces S_1 and S_5

Eq. (2.34) becomes

$$EIv = \frac{S_2 x^3}{6} - \frac{S_3 x^2}{2} - \frac{S_2 \phi x L^2}{12} + (1+\phi)\frac{L^3 S_2}{12} \tag{2.37}$$

Where

$$S_3 = \frac{S_2 L}{2} \qquad \text{and} \tag{2.38}$$

$$\phi = \frac{12EI}{GA_s L^2} \tag{2.39}$$

It should be noted here that the boundary condition for the built-in end in the engineering theory of bending when shear deformations v_s are included is taken as $dv_b/dx = 0$; that is, slope due to bending deformation is equal to zero. The remaining forces acting on the beam can be determined from the equations of equilibrium; thus we have

$$S_5 = S_2 \tag{2.40}$$

and

$$S_6 = -S_3 + S_2 L \tag{2.41}$$

Now at x = 0, v = u_2, and hence from Eq. (2.37)

$$u_2 = (1+\phi)\frac{L^3 S_2}{12EI} \tag{2.42}$$

Using Equations. (2.38), and (2.40) to (2.42), to have

$$k_{2,2} = \frac{12EI}{(1+\phi)L^3} \tag{2.43}$$

$$k_{3,2} = \frac{6EI}{(1+\phi)L^2} \tag{2.44}$$

$$k_{5,2} = -\frac{12EI}{(1+\phi)L^3} \tag{2.45}$$

$$k_{6,2} = \frac{6EI}{(1+\phi)L^2} \tag{2.46}$$

Similarly, if the left-hand end of the beam is built-in, as shown in Fig2.5b, then by use of the differential equations for the beam deflections or the condition of symmetry it can be demonstrated that

$$k_{5,5} = k_{2,2} = \frac{12EI}{(1+\phi)L^3} \tag{2.47}$$

$$k_{6,5} = -k_{3,2} = -\frac{6EI}{(1+\phi)L^2} \tag{2.48}$$

Bending Moments (S_3 AND S_6)

In order to determine the stiffness coefficients associated with the rotations u_3 and u_6 the beam is subjected to bending moments and the associated shears, as shown in Fig. 2.6a and b. The deflections can be determined from Eq. (2.34), but the constants C_1 and C_2 in these equations must now be evaluated from a different set of boundary conditions. With the boundary conditions (Fig. 2.6a)

$$v = 0 \qquad \text{at} \quad x = 0, \quad x = L \tag{2.49}$$

and

$$\frac{dv}{dx} = \frac{dv_s}{dx} = \frac{-S_2}{GA_S} \qquad \text{at x = L} \tag{2.50}$$

Eq. (2.34) becomes

$$EIv = \frac{S_2}{6}\left(x^2 - L^2 x\right) + \frac{S_6}{2}\left(Lx - x^2\right) \tag{2.51}$$

and

$$S_2 = \frac{6S_6}{(4+\phi)L} \tag{2.52}$$

As before, the remaining forces acting on the beam can be determined from the equations of equilibrium, i.e., Eqs. (2.40) and (2.41).

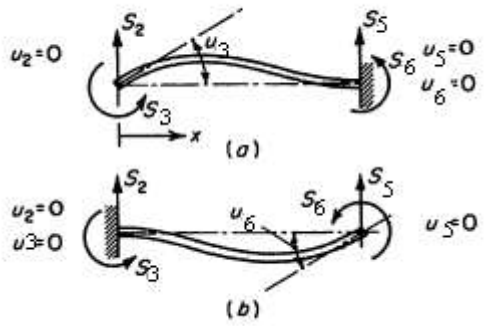

Figure 2.6 Bending moments S_3 and S_6.

Now at x = 0

$$\frac{dv_b}{dx} = \frac{dv}{dx} - \frac{dv_s}{dx} = u_3 \tag{2.53}$$

So that

$$u_3 = \frac{S_3(1+\phi)L}{EI(4+\phi)} \tag{2.54}$$

Hence from Eqs. (2.40), (2.41), (2.52) and (2.54)

$$k_{3,3} = \frac{(4+\phi)EI}{(1+\phi)L} \tag{2.55}$$

$$k_{5,3} = -\frac{6EI}{(1+\phi)L^2} \tag{2.56}$$

$$k_{6,3} = \frac{(2-\phi)EI}{(1+\phi)L} \tag{2.57}$$

If the deflection of the left-hand end of the beam is equal to zero, as shown in Fig. 2.6b, it is evident from symmetry that

$$k_{6,6} = k_{3,3} = \frac{(4+\phi)EI}{(1+\phi)L} \tag{2.58}$$

The results obtained in these subsections can now be compiled into a matrix equation relating the element forces to their corresponding displacements in the presence of temperature gradients across the beam cross section. This relationship is given by

(2.59)

$$k_e = \begin{bmatrix} \frac{EA}{L} & 0 & 0 & -\frac{EA}{L} & 0 & 0 \\ 0 & \frac{12EI}{L^3(1+\phi)} & \frac{6EI}{L^2(1+\phi)} & 0 & \frac{-12EI}{L^3(1+\phi)} & \frac{6EI}{L^2(1+\phi)} \\ 0 & \frac{6EI}{L^2(1+\phi)} & \frac{(4+\phi)EI}{L(1+\phi)} & 0 & \frac{-6EI}{L^2(1+\phi)} & \frac{(2-\phi)EI}{L(1+\phi)} \\ -\frac{EA}{L} & 0 & 0 & \frac{EA}{L} & 0 & 0 \\ 0 & \frac{-12EI}{L^3} & \frac{-6EI}{L^2(1+\phi)} & 0 & \frac{12EI}{L^3(1+\phi)} & \frac{-6EI}{L^2(1+\phi)} \\ 0 & \frac{6EI}{L^2(1+\phi)} & \frac{(2-\phi)EI}{L(1+\phi)} & 0 & \frac{-6EI}{L^2(1+\phi)} & \frac{(4+\phi)EI}{L(1+\phi)} \end{bmatrix}$$

If the shear deformations are neglected, that is, ($\phi = 0$), the stiffness matrix in (2.59) simplifies to

$$\begin{matrix} U_1 & V_1 & \theta_1 & U_2 & V_2 & \theta_2 \end{matrix} \tag{2.60}$$

$$k_e = \begin{bmatrix} \frac{EA}{L} & 0 & 0 & -\frac{EA}{L} & 0 & 0 \\ 0 & \frac{12EI}{L^3} & \frac{6EI}{L^2} & 0 & \frac{-12EI}{L^3} & \frac{6EI}{L^2} \\ 0 & \frac{6EI}{L^2} & \frac{4EI}{L} & 0 & \frac{-6EI}{L^2} & \frac{2EI}{L} \\ -\frac{EA}{L} & 0 & 0 & \frac{EA}{L} & 0 & 0 \\ 0 & \frac{-12EI}{L^3} & \frac{-6EI}{L^2} & 0 & \frac{12EI}{L^3} & \frac{-6EI}{L^2} \\ 0 & \frac{6EI}{L^2} & \frac{2EI}{L} & 0 & \frac{-6EI}{L^2} & \frac{4EI}{L} \end{bmatrix}$$

2.2 Nonlinear Analysis

In order to approach the real behavior of the structure, rather than the approximate solutions with linear analysis, nonlinear analysis is preferred. In nonlinear analysis the structure will not regain its original shape after the removal of load. Its geometry will changes resulting in stiffness change.

We fortunate that so many practical problems can be solved by so simple an approximation. However, any of the convenient assumptions that leads to a linear analysis may be at odds with reality. Adjacent parts may make or break contact. A contact area may change as load changes. Elastic material may be come plastic, or the material may not have a linear stress- strain relation at stress beyond elastic limit. Part of the structure may lose stiffness because of buckling or failure of the material. Displacement and rotations may be come large enough that equilibrium equation must be written for the deformed configuration rather than the original configuration. Large rotation caused pressure loads to change in direction, also to change in magnitude if there is a change in the area to which they are applied. Thus, for various reasons, problem may be come nonlinear [6].

Based on source of nonlinearities [7]grouped various non-linear problems in finite element analysis into the following three categories.

1. Material Non-Linearity Problems

2. Geometric Non-Linearity Problems and

3. Both material and Geometric Non-linearity Problems.

In addition to the above source of nonlinearities [8] adds boundary condition nonlinearity problem, which accounts for changes in boundary conditions with respect to structural deformation. One example of boundary condition nonlinearity is structural interaction.

2.2.1 Material Non-Linearity

When addressing the issue of material nonlinearity, one must first define the materials that one is analyzing and the variables that lead to those nonlinearities. The two most widespread materials in structural engineering are concrete and steel. The first has a

well-known brittle behavior, with very dissimilar responses for tension and compression [9].

The stress-strain relation for the material i.e. the constitutive law may not be linear and may be some times time-dependent too. For example, for concrete actual stress strain curve is as shown in Fig.2.7. Even for steel, if one is interested to study the actual behavior of the structure beyond yielding, the stress strain relation is non-linear. Hence Young's Modulus depends upon the deformation. Apart from these basic nonlinear relations, there are time dependent complex constitutive relations like plasticity, creep which make the problem non-linear. The Hognestad parabola, as shown in Figure 2.7, is a simple compression response curve, suitable for normal concrete strengths (<40 MPa).

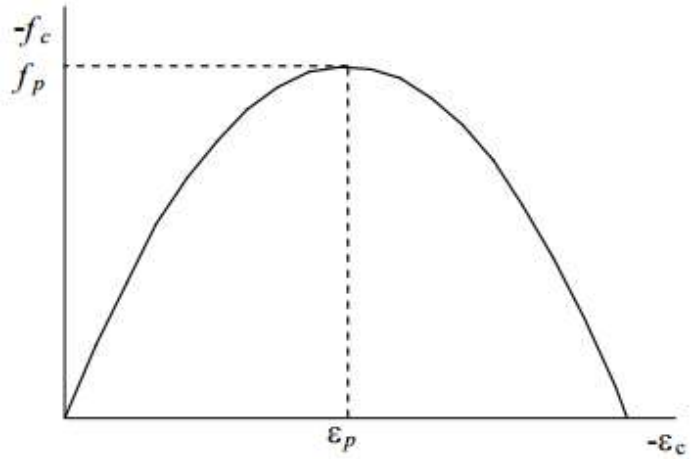

Figure 2.7 Hognestad parabolic pre- and post-peak concrete compression response

2.2.2 Geometric Non-Linearity

In many problems strains – displacement relations are not linear. They need consideration of actual strain displacement relations rather than the linear strain displacement. If a structure experiences large deformations, its changing geometric configuration can cause the structure to respond nonlinearly. Geometric nonlinearity is characterized by large displacements or rotations. It arises due to the lateral loading also and this stretching leads to a nonlinear relationship between the strain and the displacement.

Nonlinearity is achieved by updating element stiffness matrices with respect to nodal displacements. The element stiffness matrix is the function of displacement.

$$[K(d)]\{d\} = \{F\} \tag{2.61}$$

Where: d is nodal displacement

[K(d)] is element stiffness matrix as a function of nodal displacement

F is force

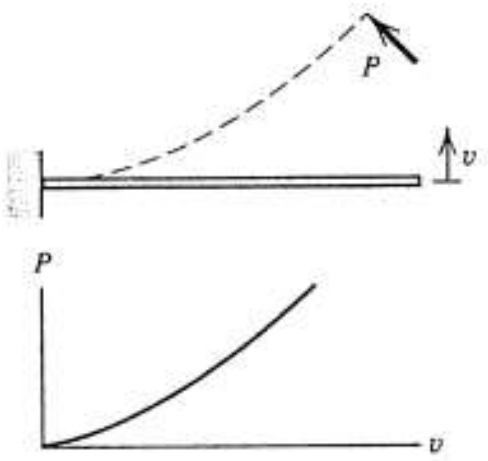

Figure 2.8 Slender elastic beam loaded by a follower force P

A simple example of geometric nonlinear problem appears in Fig. 2.8 a slender beam is loaded by a force P that acts normal to the beam axis at all times. This is an instance of a "follower force". The displacement shown is intended to represent actual displacement, not the scaling up of a linear small-displacement solution. In this case nonlinearity is geometric, meaning that nonlinearity arise s because of significant changes in the geometry of the structure [6].

Geometric nonlinearities are a common effect that is present in a wide range of fields. In a structural sense, they assume an important role when elements are subjected to compression forces, for they lead to a loss in stiffness in the elements of the structure, and, as such, should be taken into account in frame design, as opposed to only performing a first-order analysis. Tension forces are not usually a problem for they lead to an increase in stiffness of the elements in the system [9].

Large deflection /geometric nonlinear/ problem it doesn't mean that necessarily large deflections occur, but rather because stresses exist which, in the presence of certain

displacements, exert a significant influence on structural deformations. The beam-column problem illustrates this typical, large deflection behavior. Existence of axial loading in the presence of bending displacements does affect the stiffness of the member. In fact, if the loading is compressive and approaches the critical value, the bending stiffness tends toward zero. Consequently, the need for an "initial stress stiffness matrix" becomes evident.

The geometrically non-linear static responses of a cantilevered beam subjected to a non-follower point load at the free end of the beam has been studied by [10]. The authors construct the finite element model of the beam by using total Lagrangian finite element model of two dimensional solid continua for a twelve-node quadratic element. The same author try to investigate the effects of the geometric non-linearity on the displacements and on the stresses by solving non-linear problem using incremental displacement-based finite element method in connection with Newton-Raphson iteration method.

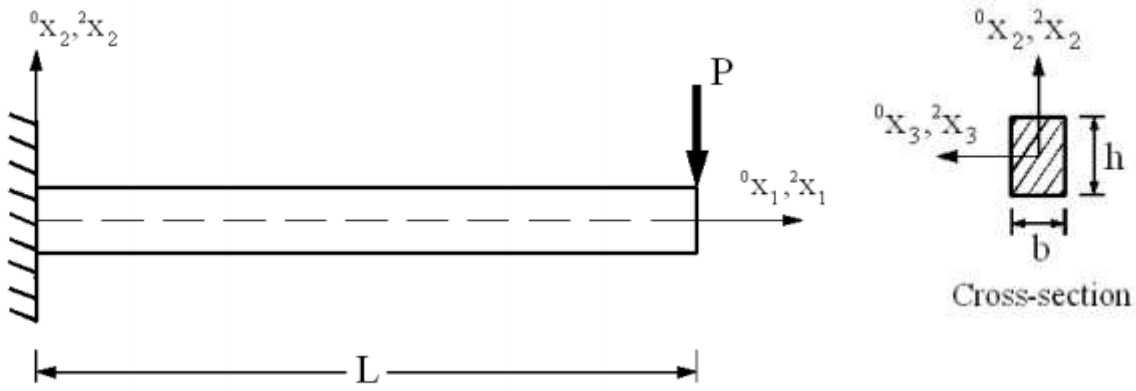

Figure 2.9 Cantilever beam subjected to a point load. [10]

[11] Presented the comparative study of linear and geometric nonlinear load-deflection behavior of beams under vertical load. In this paper a three nodded steel beam is formulated for linear and nonlinear analysis.

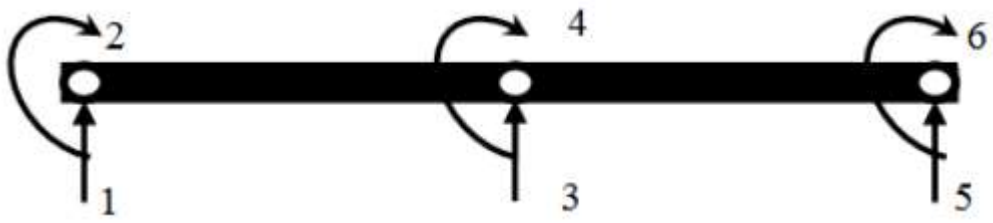

Figure 2.10 Degree of Freedom of the Beam Elements. [11]

The incremental central point load is applied to the beam. Linear and geometrically nonlinear deflection is computed for the beams. Three beams of the same length were taken for analysis, but having different thickness & support conditions. The linear and geometrical nonlinear load-deflection behavior is studied using STAAD PRO. The linear deflection is also computed by developing a finite element based code using MATLAB. The author concluded that thickness of beams significantly affect the behavior of beams. The percentage variation of linear and nonlinear deflection is very high for beam with lesser depth. Support conditions affect variation of deflection between linear and nonlinear considerably.

2.3 Material Nonlinear analysis

2.3.1 Composite Material Stiffness Matrix

In the most general case, total strains, $[\varepsilon] = [\varepsilon_x, \varepsilon_y, \gamma_{xy}]^T$, are comprised of net concrete strains $[\varepsilon_c]$, elastic strain offsets $[\varepsilon^o{}_c]$ (due to thermal, prestrains, shrinkage and lateral expansion effects), plastic strain offsets in the concrete, $[\varepsilon_c{}^p]$, (due to cyclic loading or damage), and strains due to crack shear slip, $[\varepsilon_s]$ (as considered by the distributed stress field model) as per [12].

$$[\varepsilon] = [\varepsilon_c] + [\varepsilon^o{}_c] + [\varepsilon^p{}_c] + [\varepsilon^s] \tag{2.62}$$

As well, compatibility relationships determine that the strain in the i^{th} smeared reinforcement component is the sum of the total strain, elastic strain offsets $[\varepsilon^o{}_s]_i$ (due to thermal and prestrain effects) and plastic strain offsets $[\varepsilon^s{}_p]_i$ (due to cyclic loading or damage):

$$[\varepsilon_s]_i = [\varepsilon] + [\varepsilon^o{}_s]_i + [\varepsilon^p{}_s]_i \tag{2.63}$$

At any point within the reinforced concrete continuum, the total strains are related to stresses [σ] by the composite material stiffness matrix, [D], as follows:

$$[\sigma] = [D][\varepsilon] - [\sigma^o] \tag{2.64}$$

The composite material stiffness matrix is the sum of the concrete material stiffness matrix, $[D_c]$, and the reinforcement component material stiffness matrices, $[D_s]_i$, as follows

$$[D] = [D_c] + \sum_{i=1}^{n} [D_s]_i \tag{2.65}$$

While the composite material stiffness matrix operates on total strains, element stresses can be directly related only to net strains of the concrete and reinforcement. Therefore, it is necessary to subtract the stress contribution of strain offsets and shear slip strains by use of the pseudo stress vector $[\sigma^o]$ calculated as follows:

$$\left[\sigma^o\right] = [D_c]\left\{\left[\varepsilon^o{}_c\right] + \left[\varepsilon^p{}_c\right] + \left[\varepsilon^s\right]\right\} + \sum_{i=1}^{n} [D_s]_i \left\{\left[\varepsilon^o{}_s\right]_i + \left[\varepsilon^p{}_s\right]_i\right\} \tag{2.66}$$

As the MCFT and DSFM model the reinforced concrete as an orthotropic material in the principal stress directions, it is necessary to formulate the concrete material stiffness matrix,$[D_c]'$, relative to these directions. If it is assumed that the Poisson's effect is negligible, then $[D_c]'$ is computed as follows:

$$[D_c] = \begin{bmatrix} \overline{E_{cl}} & 0 & 0 \\ 0 & \overline{E_{c2}} & 0 \\ 0 & 0 & \overline{G_c} \end{bmatrix} \tag{2.67}$$

The secant moduli $\overline{E_{c1}}$, $\overline{E_{c1}}$,$\overline{G_c}$, as shown in Figure 8, are computed from the current values of the principal stresses, f_{c1} and f_{c2}, and the corresponding principal net concrete strains, ε_{c1} and ε_{c2}, as follows:.

$$\overline{E_{c1}} = \frac{f_{c1}}{\varepsilon_{c1}}; \overline{E_{c2}} = \frac{f_{c2}}{\varepsilon_{c2}}; \overline{G_c} = \frac{\overline{E_{c1}} \ * \ \overline{E_{c2}}}{\overline{E_{c1}} \ + \ E_{c2}} \tag{2.68}$$

Likewise, material stiffness matrices $[Ds]_{i'}$ for each reinforcement component must first be determined relative to their longitudinal axes. As the reinforcement is assumed only to resist uniaxial stresses, $[Ds]_{i'}$ is computed as follows:

$$[D_s]_i' = \begin{bmatrix} \overline{\rho_i E_{si}} & 0 & 0 \\ 0 & 0 & 0 \\ 0 & 0 & 0 \end{bmatrix} \tag{2.69}$$

where ρ_i is the reinforcement ratio of the reinforcement component. The secant modulus $\overline{E_{si}}$, as shown in Figure 2.11, is computed from its current value of stress, f_{si} and the corresponding strain, ε_{si} as follows:

$$\overline{E_{si}} = \frac{f_{si}}{\varepsilon_{si}} \tag{2.70}$$

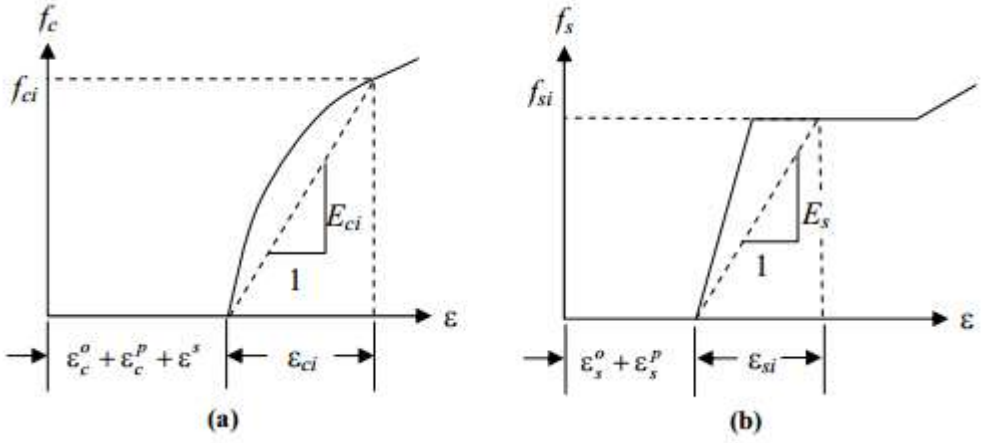

Figure 2.11 Definition of secant moduli for a) concrete b) reinforcement [12]

Likewise, in the case of FRC, the material stiffness matrix for fibers can be determined based on the net strains in the direction of the crack. The fibre material stiffness matrix, $[D_f]'$, is computed as follows:

$$\left[D_f\right]' = \begin{bmatrix} \overline{E_{fl}} & 0 & 0 \\ 0 & 0 & 0 \\ 0 & 0 & 0 \end{bmatrix} \tag{2.71}$$

The secant modulus, $\overline{E_{f1}}$, is computed from the tensile stress attained by fibres which is averaged between cracks and from the strain:

$$\overline{E_{fi}} = \frac{\alpha_{avg} f_f}{\varepsilon_{cf}} \tag{2.72}$$

$$\varepsilon_{cf} = \frac{\varepsilon_{c1} + \varepsilon_{c2}}{2} + \frac{\varepsilon_{c1} - \varepsilon_{c2}}{2} \cos 2\theta_f \tag{2.73}$$

$$\theta_f = \tan^{-1} \frac{\delta_s}{w_{cr}} \tag{2.74}$$

The material stiffness matrices, $[D_c]'$, $[D_f]'$, and $[D_s]'_i$, are transformed from their respective principal axes to the x,y axes by means of the transformation matrix, [T], as follows:

$$[D_c] = [T_c]^T [D_c]' [T_c] + [T_f]^T [D_f]' [T_f] \tag{2.75}$$

where $[T_c]$ is calculated using θ_σ, and $[T_f]$ is calculated using $\theta_\sigma + \theta_f$, and:

$$[D_s]_i = [T_s]_i^T [D_s]'_i [T_s] \tag{2.76}$$

$$[T] = \begin{bmatrix} \cos^2\psi & \sin^2\psi & \cos\psi\sin\psi \\ \sin^2\psi & \cos^2\psi & -\cos\psi\sin\psi \\ -2\cos\psi\sin\psi & 2\cos\psi\sin\psi & \left(\cos^2\psi - \sin^2\psi\right) \end{bmatrix} \tag{2.77}$$

For the concrete, the angle ψ is the inclination of the principal tensile stress axis, θσ, with respect to the positive x-axis. For the fibres, the angle ψ is the inclination of the principal tensile stress axis, $\theta_\sigma+\theta_f$ with respect to the positive x-axis. For the reinforcement, the angle ψ is the orientation, αi, of each reinforcement component, with respect to the positive x-axis.

2.3.2 Element Stiffness Matrices

The element stiffness matrix, [k] relates nodal forces to nodal displacements of the element. It is determined from the composite material stiffness matrix as follows:

$$[k] = \int_{vol} [B]^T [D][B] dv \tag{2.78}$$

The strain-displacement matrix [B], interpolates strains throughout the element continuum by operating on nodal displacements of the element. The form of the strain displacement matrix depends on the type of the element, and the resulting value of the above integration will depend on the composite material stiffness matrix, the element geometry and the exactness of the integration method. It is also possible to separate the element stiffness matrix into contributions from the stiffness of the concrete, $[k_c]$, and stiffness of the reinforcement components, $[k_s]_i$, by substituting the respective material stiffness matrix for the composite material stiffness matrix:

$$[k_c] = \int_{vol} [B]^T [D_c][B] dv \tag{2.79}$$

$$[k_s]_i = \int_{vol} [B]^T [D_s]_i [B] dv \tag{2.80}$$

2.4 Geometric Nonlinear Analysis

Geometric nonlinearity occurs when the deflections are large enough to cause significant changes in the geometry of the structure, so that the equations of equilibrium must be formulated for the deformed configuration. The general goal of analysis is to construct the nonlinear relation between applied load and the resulting deformation.

2.4.1 Strain Energy

Considering a uniform section prismatic element, Fig.2.3, subjected to axial and flexural deformation (no shear), the Lagrangian finite strain-displacement relation is given by, from linear analysis,

$$\varepsilon_{xx} = u_x + \frac{1}{2}\left(u^2{}_{,x} + v^2{}_{,x} + w^2{}_{,x}\right) \tag{2.81}$$

Thus, the total strain would be

$$\varepsilon_{xx} = \frac{du}{dx} - y\left(\frac{d^2v}{dx^2}\right) + \frac{1}{2}\left(\frac{dv}{dx}\right)^2 \tag{2.82}$$

Axial *Flexure* *Large Deformation*

We note that the first and second terms are the familiar components of axial and flexural strains respectively, and the third one (which is nonlinear) is obtained from large-deflection strain-displacement.

The Strain energy of the element is given by

$$U^e = \frac{1}{2}\int_v E\varepsilon^2{}_{xx}\,dv \tag{2.83}$$

Substituting Eq2.82 into U^e to obtain

$$U^e = \frac{1}{2}\int_L \left[\begin{array}{l}\left(\frac{du}{dx}\right)^2 + y^2\left(\frac{d^2v}{dx^2}\right)^2 + \frac{1}{4}\left(\frac{dv}{dx}\right)^2 - 2y\left(\frac{du}{dx}\right)\left(\frac{d^2v}{dx^2}\right) - \\ y\left(\frac{d^2v}{dx^2}\right)\left(\frac{dv}{dx}\right)^2 + \left(\frac{du}{dx}\right)\left(\frac{dv}{dx}\right)^2\end{array}\right] dA\,dx \tag{2.84}$$

Note that $\int_A dA = A, \qquad \int_A y\,d_A = 0; \qquad \int_A y^2 d_A = I$

For y measured from the centroid, U^e reduces to

$$U^e = \frac{1}{2}\int_L E\left[A\left(\frac{du}{dx}\right)^2 + I\left(\frac{d^2v}{dx^2}\right)^2 + \frac{A}{4}\left(\frac{dv}{dx}\right)^4 + A\left(\frac{du}{dx}\right)\left(\frac{dv}{dx}\right)^2\right] dx \tag{2.85}$$

We discard the highest order term, $\frac{A}{4}\left(\frac{dv}{dx}\right)^4$ in order to transform the above equation into a linear instability formulation.

Under the assumption of an independent pre buckling analysis for axial loading, the axial load P_x is

$$Px = EA\frac{du}{dx} \tag{2.86}$$

Thus Eq. 2.85 reduces to

$$U^e = \frac{1}{2}\int_L \left[EA\left(\frac{du}{dx}\right)^2 + EI\ \left(\frac{d^2v}{dx^2}\right)^2 + Px\left(\frac{dv}{dx}\right)^2 \right] dx \tag{2.87}$$

It can be thus decoupled the strain energy into two components, one associated with axial and the other with flexural deformations

$$U^e = U_a{}^e + U_f{}^e \tag{2.88a}$$

$$U_f{}^e = \frac{1}{2}\int_L \left[EI\left(\frac{d^2v}{dx^2}\right)^2 + Px\left(\frac{dv}{dx}\right)^2 \right] dx \tag{2.88b}$$

2.4.2 Potential Energy

Model body by dividing it into an equivalent system of many smaller bodies or units (finite elements discretization) interconnected at points common to two or more elements (nodes or nodal points) and/or boundary lines and/or surfaces.

Assuming a functional representation of the transverse displacements in terms of the four joint displacements

$$\mathrm{v} = \mathrm{N}\,\bar{u} \tag{2.89a}$$

$$\frac{dv}{dx} = \mathrm{N}_{,x}\,\bar{u} \tag{2.89b}$$

$$\frac{\mathrm{d}^2\mathrm{v}}{\mathrm{dx}^2} = N_{,xx}\bar{u} \tag{2.89c}$$

Substituting this last equation into Eq.2.88b, the element potential energy is given by

$$\Pi^e = U_f{}^e + W^e \tag{2.90a}$$

$$= \frac{1}{2}\lfloor \overline{u_e} \rfloor [ke] \{\bar{u}_e\} + \frac{1}{2}\lfloor \overline{u_e} \rfloor [kg] \{\bar{u}_e\} - \lfloor \bar{u} \rfloor \{p\} \quad (2.90b)$$

Where

$$[ke] = \left[\int_L EA\{N, xx\}\lfloor N, xx \rfloor dx\right] \quad (2.91\&2.92)$$
$$[kg] = \left[P\int_L \{N, x\}\lfloor N, x \rfloor dx\right]$$

Where [ke] is the conventional element flexural stiffness matrix.

[kg] introduces the considerations related to elastic instability. It is noted that its terms in addition to axial load depend on geometric parameters (length), therefore this matrix is often referred to as the geometric stiffness matrix.

From linear analysis we have shape function given in Eq.2. 17a – 2.17d

Using the shape functions for flexural elements, Eq.2. 17a – 2.17d, and substituting into Eq. 2.91 and Eq. 2.92 to obtain

$$k_e = \begin{matrix} U_1 \\ V_1 \\ \theta_1 \\ U_2 \\ V_2 \\ \theta_2 \end{matrix} \begin{bmatrix} \frac{EA}{L} & 0 & 0 & -\frac{EA}{L} & 0 & 0 \\ 0 & \frac{12EI}{L^3} & \frac{6EI}{L^2} & 0 & \frac{-12EI}{L^3} & \frac{6EI}{L^2} \\ 0 & \frac{6EI}{L^2} & \frac{4EI}{L} & 0 & \frac{-6EI}{L^2} & \frac{2EI}{L} \\ -\frac{EA}{L} & 0 & 0 & \frac{EA}{L} & 0 & 0 \\ 0 & \frac{-12EI}{L^3} & \frac{-6EI}{L^2} & 0 & \frac{12EI}{L^3} & \frac{-6EI}{L^2} \\ 0 & \frac{6EI}{L^2} & \frac{2EI}{L} & 0 & \frac{-6EI}{L^2} & \frac{4EI}{L} \end{bmatrix} \quad (2.93)$$

which is the same element stiffness matrix derived earlier in Eq. 2.60

The geometric stiffness matrix is given by

$$k_g = \frac{P}{L} \begin{matrix} \\ \\ \\ \\ \\ \\ \end{matrix} \begin{matrix} U_1 & V_1 & \theta_1 & U_2 & V_2 & \theta_2 \end{matrix} \begin{bmatrix} 0 & 0 & 0 & 0 & 0 & 0 \\ 0 & \frac{6}{5} & \frac{4}{10} & 0 & \frac{-6}{5} & \frac{L}{10} \\ 0 & \frac{L}{10} & \frac{2L^2}{15} & 0 & \frac{-L}{10} & \frac{-L^2}{30} \\ 0 & 0 & 0 & 0 & 0 & 0 \\ 0 & \frac{-6}{5} & \frac{-L}{10} & 0 & \frac{6}{5} & \frac{-L}{10} \\ 0 & \frac{L}{10} & \frac{-L^2}{30} & 0 & \frac{-L}{10} & \frac{2L^2}{15} \end{bmatrix} \quad (2.94)$$

The equilibrium relation is thus

$$K\bar{}_u = \overline{P} \tag{2.95}$$

In a global formulation, we would have

$$K = K_e + K_g \tag{2.96}$$

We note that the structure becomes stiffer for tensile load *P* applied through **K***g*, and weaker in compression.

$$K_g = \lambda K_g * \tag{2.97}$$

Where K_g* corresponds to the geometric stiffness matrix for unit values of the applied loading ($\lambda = 1$).

The elastic stiffness matrix **K***e* remains a constant, hence we can write

$$\left(K_e + \lambda K_g *\right)\bar{u} - \lambda\overline{P*} = 0 \tag{2.98}$$

The displacements are in turn given by

$$\bar{u} = \left(K_e + \lambda K_g *\right)^{-1} \lambda\overline{P*} \tag{2.99}$$

and for the displacements to tend toward infinity (i.e. buckling/bifurcation/instability), then

$$\left|K_e + \lambda K_g *\right| = 0 \tag{2.100}$$

which can also be expressed as

$$\left|K_g{}^{-1}K_e + \lambda I\right| = 0 \tag{2.101}$$

Alternatively, it can simply be argued that there is no unique solution (bifurcation condition) to **u**.

The lowest value of λ, $\lambda crit$ will give the buckling load for the structure and the buckling loads will be given by

$$\overline{P_{cr}} = \lambda_{cr}\,\overline{P*} \tag{2.102}$$

The corresponding deformed shape is directly obtained from the corresponding eigenvector.

2.4.4 Second-Order Elastic Analysis

From Eq. 2.94 it is evident that since *kg* depends on the magnitude of *Px*, which itself may be an unknown in a framework, then we do have a *geometrically non-linear* problem.

We rewrite Eq. 2.96 as

$$\left[K_e + K_g\right]\bar{u} = \bar{P} \tag{2.103}$$

but since **K***g* depends on the axial load *P*, the problem is nonlinear. A simple way to solve this nonlinear equation is to use a step-by-step incremental procedure. The linearized incremental formulation can be obtained by applying an incremental operator Δ.

$$\left\{\bar{P}\right\}_i = \left[K_e + K_g\right]_{i-1}\left\{\bar{u}\right\}_i \tag{2.104}$$

2.5 Effect of Axial load on Flexural Deformation

So many literatures have been conducted on the flexural design method and flexural design theorems of RC members. [13] Derived three theorems of the flexural theory for RC members to identify two critical points on a moment–curvature curve: (1) the onset of flexural strength and (2) the onset of the so-called true ultimate curvature. The true ultimate curvature is reached at the exact moment when a RC member loses its integrity. Three theorems are derived for RC flexural behavior: one for the flexural strength of under reinforced members (reinforcement yields before the onset of the peak moment), another for that of general flexural members, and a third for the evaluation of ultimate deformation. In this literature the theorems are derived for RC members with a constant axial load.

Members carrying both axial force and bending moment are subjected to an interaction between these effects. The analysis of a beam-column using stability functions as an alternative to the stress stiffness matrix is discussed by [14]. In this literature the Authors derive an explicit expressions for stability functions for three-dimensional beam-columns, in terms of member length, cross-sectional properties, axial force, and the end moments. The effect of flexure on axial stiffness and the effect of axial force on flexural stiffness and stiffness against translation are considered in the derivation of stability

functions. The nonlinear stiffness matrix of a three dimensional beam-column using the stability functions is presented by modifying the linear elastic stiffness matrix for a beam-column (which includes the effect of shear deformations) available in the literature.

The authors outlined the theoretical considerations for the derivation of stability functions s_l to s_9, where s_1 = stability function for the effect of flexure on axial stiffness; s_2 = stability function for the effect of axial force on flexural stiffness against rotation of near end about z-axis; s_3 = stability function for the effect of axial force on flexural stiffness against rotation of far end about z-axis; s_4 = stability function for the effect of axial force on flexural stiffness against rotation of near end about y-axis; s_5 = stability function for the effect of axial force on flexural stiffness against rotation of far end about y-axis; s_6 = stability function for the effect of axial force on flexural stiffness (about z-axis) against translation in y-direction; s_7 = stability function for the effect of axial force on shear stiffness in y-direction against translation in y-direction; s_8 = stability function for the effect of axial force on flexural stiffness (about y-axis) against translation in z direction; and s_9 -stability function for the effect of axial force on shear stiffness in z-direction against translation in z-direction. The effect of axial force on torsional stiffness and the effect of torsional moment on axial stiffness are neglected in the theoretical formulation.

The axial stiffness of the beam in the absence of end moments is given by EA/l, and the axial deformation due to axial load P is given by Pl/EA. However, the end moments produce an additional axial deformation in the beam. In order to include the effect of flexure on axial deformation, the axial stiffness of the beam-column must be modified. Let the modified axial stiffness be s_1 (EA/l) where s, is the modification factor or the stability function for the effect of flexure on axial stiffness. Then the authors derived an expression for s_1.

(a)

(b)

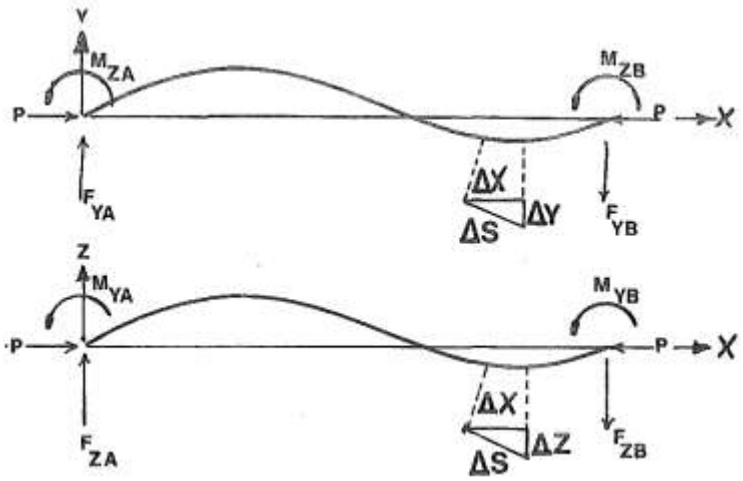

Figure 2.12 Effect of Flexure on Axial Stiffness: (a) Bending in *X-Y* plane; *(b)* Bending in *X-Z* plane [14]

The stability function s_2, s_3 and s_4, s_5, which are corresponding to the effect of axial force on flexural stiffness against rotation, have been derived using the differential equation of the beam-column bending in the X-Y plane, Fig.2.12 (a), and X-Z plane, Fig.2.12 (b), respectively. Similarly the function s_6, s_7, s_8, and s_9, which are corresponding to the effect of axial force on flexural stiffness against translation, have been derived using the slope-deflection equation.

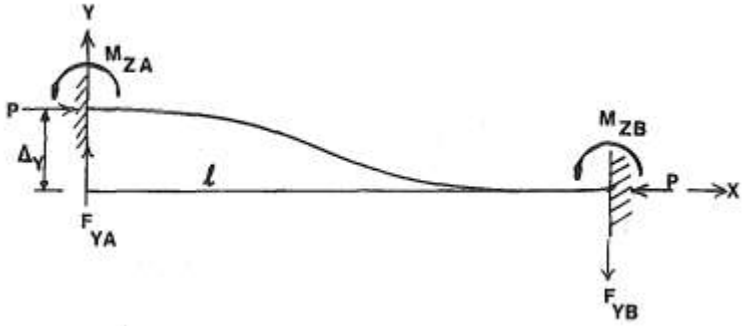

Figure 2.13 Effect of Axial Force on Stiffness against Translation [14]

The lateral deflection of a member causes additional bending moment when subjected to a simultaneously applied axial force. This alters the flexural stiffness of the member. In a like manner, the presence of bending moments affects the axial stiffness of the member due to an apparent shortening of the member caused by the bending deformations. If the

deformations are small, the interaction between bending and axial forces can be ignored, in which case the force deformation relationship for a beam-column is given by Eq.1.1.

The problem of a concrete cross section under flexural and axial loading is indeterminate due to the existence of more unknowns than equations. Among the infinite solutions, it is possible to find the optimum, which is that of minimum reinforcement that satisfies certain design constraints (section ductility, minimum reinforcement area, etc.). In the design of members under combined flexure and axial load it is common to use conventional methods to obtain the reinforcement with symmetrical distribution. This may be appropriate in some cases of flexural moments with different signs and similar values. However, in other cases this distribution may result in uneconomical constructive simplification and be environmentally inadequate, with it being more interesting not to use the symmetrical distribution, but to search for another distribution with optimum reinforcement [15].

The author proposed the automation of the optimum reinforcement calculation under any combination of flexural and axial loading. The procedure has been implemented in a program code. According to the literature when solving the problem of optimum reinforcement what is mainly achieved is automating, with a negligible computational time, the reinforcement calculation of a cross section subjected to flexural and axial loading. Moreover, when observing the graphical results, particularly the depth of neutral axis, the physical sense of the problem can be visualized, since the stress-strain state of the section is known instantly.

[16] Carried out geometrical nonlinear analysis of the prismatic plane frames using the stability functions and updating the stiffness matrix in every iteration. At the first stage of the analysis the author assumed that the axial forces acting on the members as zero, and then, the system was solved linearly under the initially set external loads, and the member axial forces were determined. The Stability Functions were calculated by using the obtained axial forces and the system was resolved under the same external loads. The operations were repeated for each iteration under the same external loads until the axial forces became constant. At the end of the iteration, the determinant and the eigenvalues of the system stiffness matrices, the system displacements and the axial forces of the members were determined. The external loads were regularly increased at the beginning of each iteration by multiplying them with a load factor of λ, or the operations were

continued until the least Eigenvalue became zero. Thus, at this stage, the critical load or buckling load of the system was found.

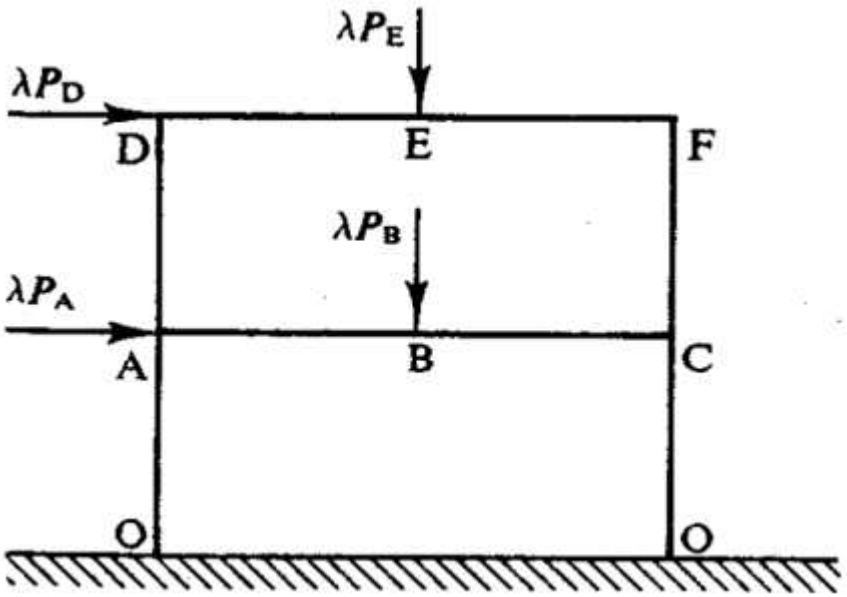

Figure 2.14 The application of λ load factor to the external load system [16]

Finite difference technique is the familiar method of identifying the buckling load of a beam-column. [17] Present a method named Multi segment Integration technique to identifying the buckling load of a structural member which is subjected simultaneously to axial compressive force and bending moment (beam-column). The different end support condition i) hinged at both ends; ii) fixed at both ends; and iii) fixed at one end and hinged at the other end were assumed as a boundary condition for the development of boundary- value problem for the beam-column equation.

The authors used a mathematical model based on the basic equation of beam-column theory which is a differential equation, linking the displacement of the center line w(x) to the axial compressive load P and the lateral load q(x). That is,

$$EI\frac{d^4w}{dx^4} + P\frac{d^2w}{dx^2} = q \tag{2.105}$$

together with the boundary condition

i) $w(0) = w''(0) = w(l)\ (= w''(l) = 0$

ii) $w(0) = w'(0) = w(l)\ (= w'(l) = 0$

iii) $w(0) = w'(0) = w(l)\ (= w''(l) = 0$

Where *E* is the Young's modulus of the beam, *I* is the area moment of inertia of the

beam's cross section.

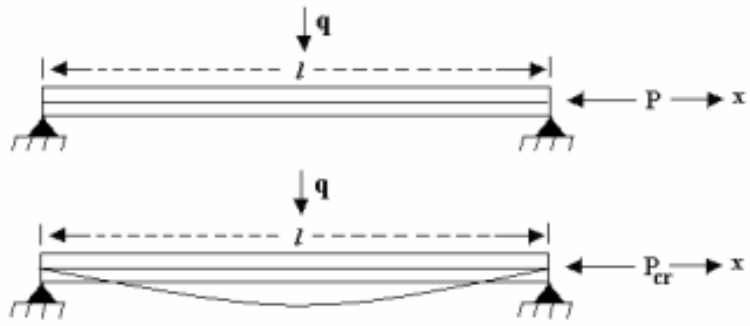

Figure 2.15(a). Beam-column with both ends hinged.

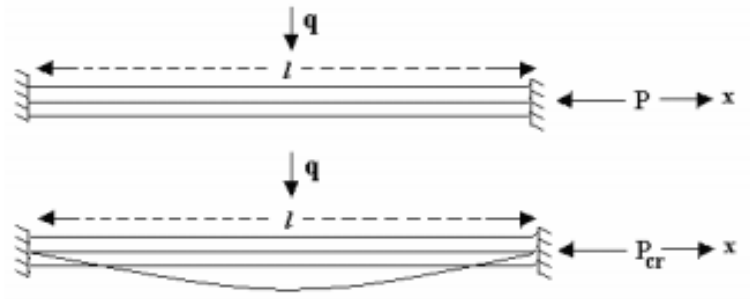

Figure 2.15(b). Beam-column with both ends fixed

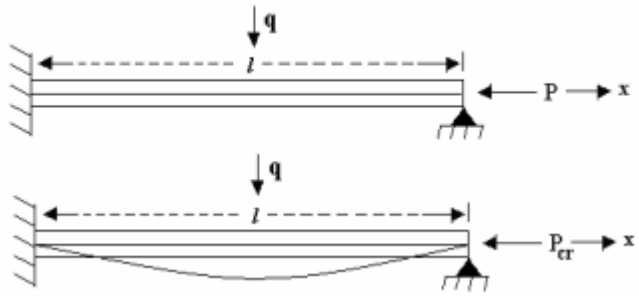

Figure 2.15 **(c).** Beam-column with one end fixed and other end hinged. [17]

The authors presented the analytical expression of the deflection equation for different boundary conditions. Then the Euler buckling load for q(x) = 0; the formulation of the fourth order non homogeneous beam-column equation using both Finite Difference method and Multi-segment Integration technique were presented. Finally they established some results on critical load and graphical presentation of buckling load obtained from Multi-segment Integration technique. Based on the result the authors have found that the Multi-segment Integration technique is seen to be capable of solving this kind of problem and that the method is both effective and efficient.

This work will focus mainly on the axial load effect on flexural deformation in linear and geometric nonlinear analysis. The percentage difference of flexural deformation in linear and geometric nonlinear analysis under incremental axial load with varied depth, length and support condition of reinforced concrete member will be investigated.

2.6 Solution Technique for Geometric Nonlinear Problems

In linear analysis of the structure there is no appreciable change in the geometry of the structure after loading. Hence the transformation matrix used to connect global and local values remained constant through and the following relations could be used:

$$\{d_g\} = [L]^T \{d\} \tag{2.106}$$

$$\{k_g\} = [L]^T \{k_e\} \{L\} and \tag{2.107}$$

$$\{F_g\} = [L]^T \{F_e\} \tag{2.108}$$

Where, subscript *g* refers to global values and *d* refers to local values. [*L*] is the rotation (transformation) matrix.

In cable structures, the deflections are large. Hence change of geometry with loads are not negligible. There are attempts to study the effect of changes in geometry on structures like shells also. Consider a bar element shown in Fig. 2.16. The line 1-2 shows initial position. After loading the element takes position 1'- 2'. Hence its inclination to global x-axis changes from **θ** to **θ+ Δ θ**. Hence the rotation matrix *L* changes. Thus *L* is not constant throughout but it is a function of displacement. We can represent this by writing $[L] = [L\{d\}]$. Hence the stiffness matrix varies with displacements. This type of non-linear problems may be handled by incremental iterative or mixed method similar to handling material non-linearity problems.

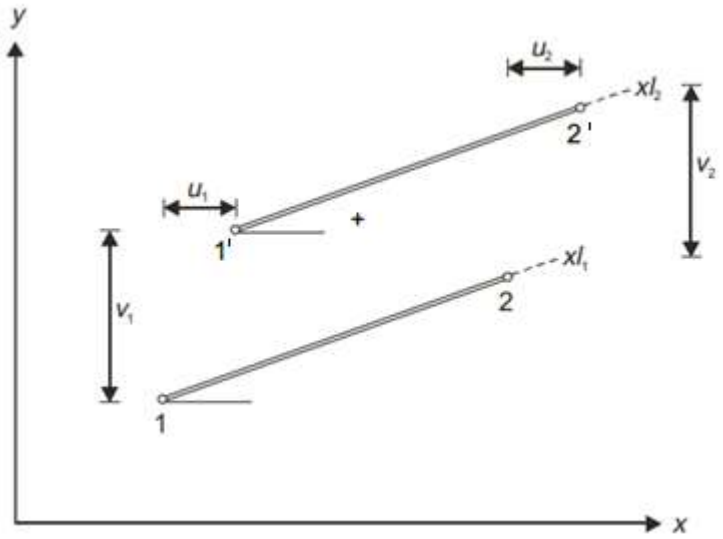

Figure 2.16 Geometric non-linearity [18]

Incremental procedure

$$\{F_g\}+\{\Delta F_g\}=([L]+[\Delta L])^T(\{F_l\}+\{\Delta F_l\})$$

$$=[L]^T\{F_l\}+[L]^T\{\Delta F_l\}+[\Delta L]^T\{F_l\}+[\Delta L]^T\{\Delta F_l\}$$

Neglecting the small quantity of higher order, the above equation will be

$$\{F_g\}+\{\Delta F_g\}=[L]^T\{F_l\}+[L]^T\{\Delta F_l\}+[\Delta L]^T\{F_l\}$$

Since $[F_g]=[L]^T\{F_l\}$, the above equation reduces to

$$\{\Delta F_g\}=[L]^T\{\Delta F_l\}+[\Delta L]^T\{F_l\} \tag{2.109}$$

From the stiffness equation, we know

$$[L]^T\{\Delta F_l\}+[k_g]\{\Delta d_g\}$$

∴ Equation 2.109 reduces to

$$\{\Delta F_g\}=[k_g]\{\Delta d_g\}+[\Delta L]^T\{F_l\} \tag{2.110}$$

In the above equation, the term $[\Delta L]^T[F_e]$ represents the change in stiffness equation due to change in the geometry. Let us consider this term further

$$[\Delta L]^T\{F_l\}=\sum_{i=1}^{n}\{F_l\}\{\Delta L\}_i \tag{2.111}$$

but

$$\Delta L_i=\frac{\partial\{L\}_i}{\partial(d_g)}(\Delta d_g)=\frac{\partial\{L\}_i}{\partial(d_g)}d_g$$

$$=\left[\frac{\partial\{L\}_i}{\partial(d_g)}_1\ \frac{\partial\{L\}_i}{\partial(d_g)}_2\ \ldots\frac{\partial\{L\}_i}{\partial(d_g)}n\right] \tag{2.112}$$

$$\therefore[\Delta L]^T\{F_e\}=\sum_{i=1}^{n}\{F_e\}_i[G_i]\{\Delta d_g\}_i$$

Substituting it in equation 2.110, to get

$$\{\Delta F_e\} = [k_g]\{\Delta d_g\} + \sum_{i=1}^{n} \{F_e\}_i [G_i]\{\Delta d_g\}$$

$$= k_g \Delta d_g + (\sum_{i=1}^{n} (F_e)_i [G_i]\{\Delta d_g\}$$

$$= [k_g + k_G]\{\Delta d_g\} \qquad (2.113)$$

Where $k_G = \sum_{i=1}^{n} (F_e)_i [G_i]$

Since it is normally talked about global values in the final analysis, for simplicity can be dropped subscript '*g*' and write equation 2.113 as

$$\{\Delta F\} = ([k] + [k_G])\{\Delta d\} \qquad (2.114)$$

From i^{th} stage, if we want to proceed to $i + 1^{nth}$ stage, the equation 2.11 is

$$([k] + [k_G])_i \{\Delta d_{i+1}\} = \Delta F_{i+1} \qquad (2.115)$$

Thus to get additional deflections due to geometric non-linearity we need stiffness matrices [*k*] and [*kG*] at the beginning of an increment. Hence evaluation effort required is more. However it may be noted that to find [*kG*] there is no need to evaluate the stiffness matrix afresh. Only modifications to transformation matrix [*L*] is needed.

Iterative procedure

This method is straight forward. For the initial geometry, the transformation matrix is assembled. Using this it is found,

$$[k_0] = [L_o]^T [k_l][L_o] \qquad (2.116)$$

$$[F_0] = [L_o]^T [F_l] \qquad (2.117)$$

Then after solving stiffness equation,

$$[k_0]\{d_1\} = [F_o] \qquad (2.118)$$

One can get d values of 1st stage. Using these displacements, the new coordinates of the nodes are determined. For the new geometry the above process is repeated to get displacements d_2 of second stage. The process is repeated until the displacements no longer change significantly. Though the process is simple, it has limitations of the iterative techniques i.e. convergence is slow. It is time consuming.

Mixed procedure

Instead of applying total load in each iteration, if we apply load in the increments and for every incremented load carryout the iterative procedure, better results may be obtained. It involves lot of computational effort.

3. Nonlinear Analysis

3.1 Nonlinear analysis of Flexural members

To check the validity of the formulation of linear and geometrical nonlinear load-deflection behavior, eight types of three nodded beams are analysed using software's. Linear behavior is carried out using STAAD Pro and by a finite element based Sci.lab code and nonlinear behavior by using STAAD Pro. For checking the effect of beam depth, length and supporting condition on linear and geometric nonlinear effect of axial load the following eight beams are considered:-

3.1.1 Simply supported beam

Material Property

f_{ck} = 25 N/mm^2 (concrete strength class C25/30)

f_{yk} =500N/mm^2 (Steel B500B)

- ✓ Simply supported RC beams with depth 200mm and length of 4m, 6m, 8m

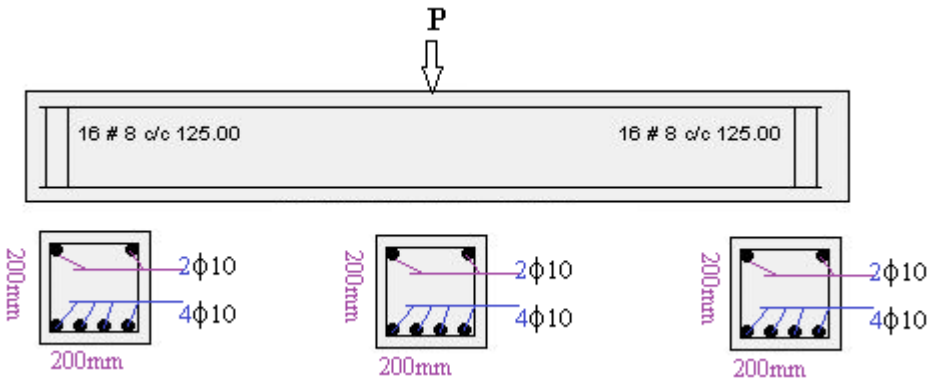

Figure 3.1 Model Type 1.

- ✓ Simply supported RC beam with depth 300mm and 8m length

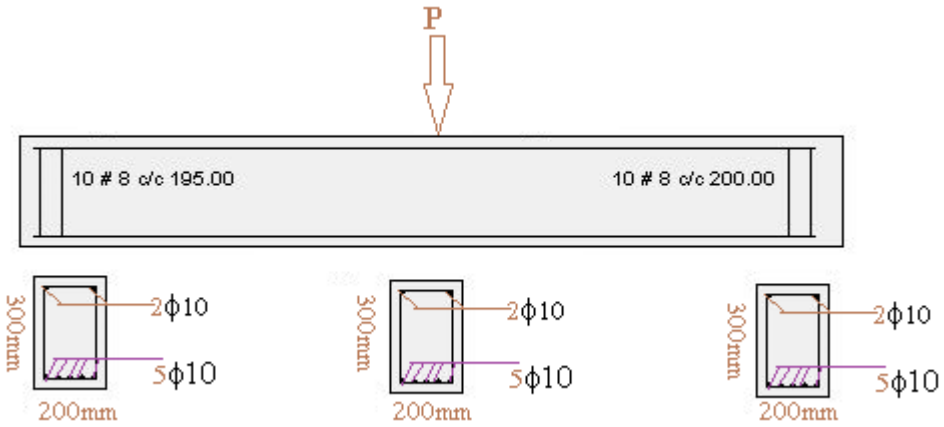

Figure 3.2 Model Type 2.

- ✓ Simply supported RC beam with one end roller support having depth of 200mm, length 6m and subjected to external axial load

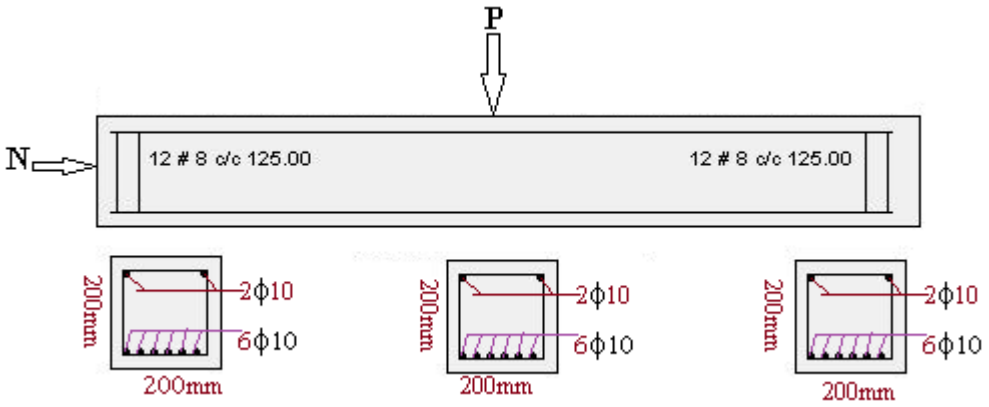

Figure 3.3 Model Type 3.

- ✓ Simply supported RC beam with one end roller support having depth of 200mm, length 6m and without external axial load

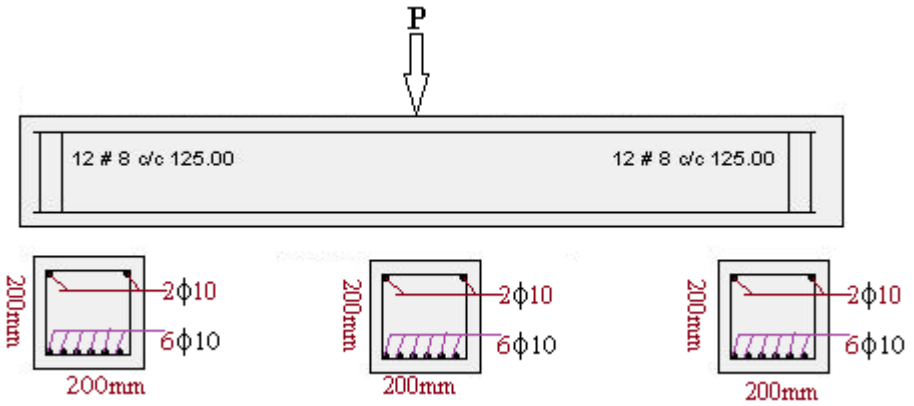

Figure 3.4 Model Type 4.

3.1.2 Fixed supported beam

Material Property

f_{ck} = 25 N/mm^2 (concrete strength class C25/30)

f_{yk} =500N/mm^2 (Steel B500B)

- ✓ Both end fixed supported RC beam with depth 200mm and 6m in length

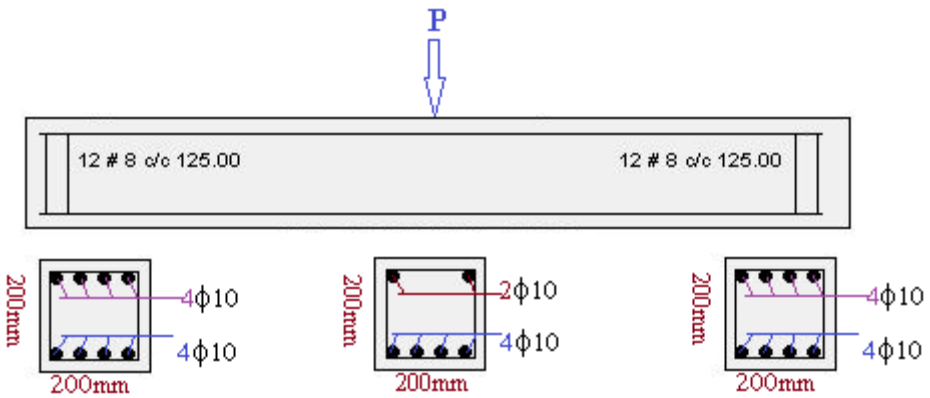

Figure 3.5 Model Type 5.

- ✓ Both end fixed supported RC beam with depth 200mm and 6m in length

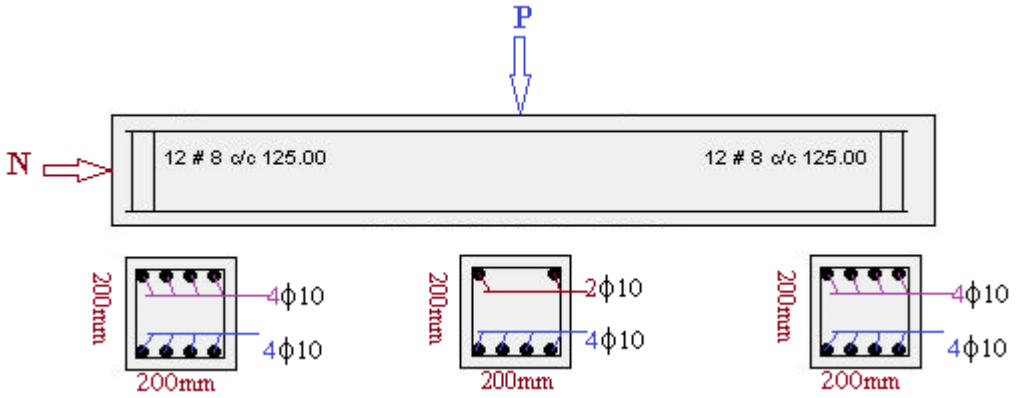

Figure 3.6 Model Type 6.

3.2 Four story RC building Frame Analysis

Four-story reinforced concrete residential building shown in Fig.3.7. The column and beam sizes are assumed as 0.2 X 0.3m and 0.3 m X 0.4m respectively.

Material Property

f_{ck} = 25 N/mm^2 (concrete strength class C25/30)

f_{yk} =500N/mm^2 (Steel B500B)

The building is analysed by equivalent static analysis procedure for getting lateral loads at each story. After getting the lateral forces load deformation behavior for linear and geometric nonlinear analysis is carried out by using STAAD PRO and ETABS 2016. Then the building frame loaded both lateral load and gravity load and linear and geometric nonlinear analysis is carried out once again. To investigate the effect of axial load in selected story beams. For nonlinear analysis deformation, load step is taken as ten which means it divide the total loads into ten increments and number of iteration is taken as 100, which is enough for getting accurate answer. In nonlinear analysis at each load increment case the tangent stiffness matrix is updating.

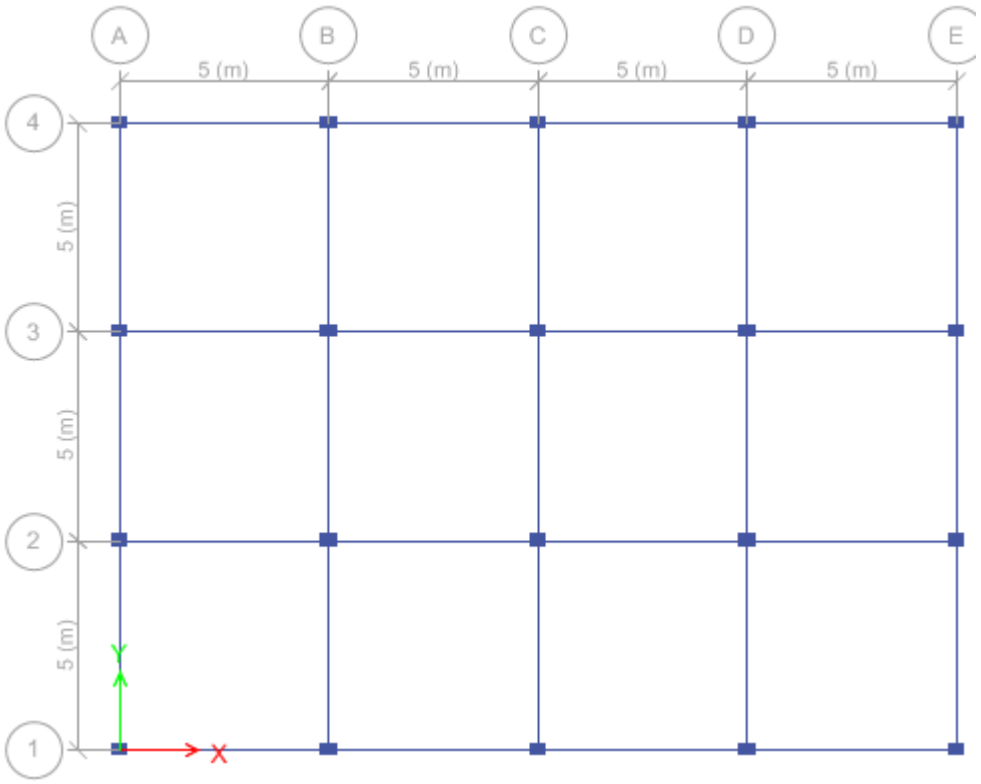

Plane

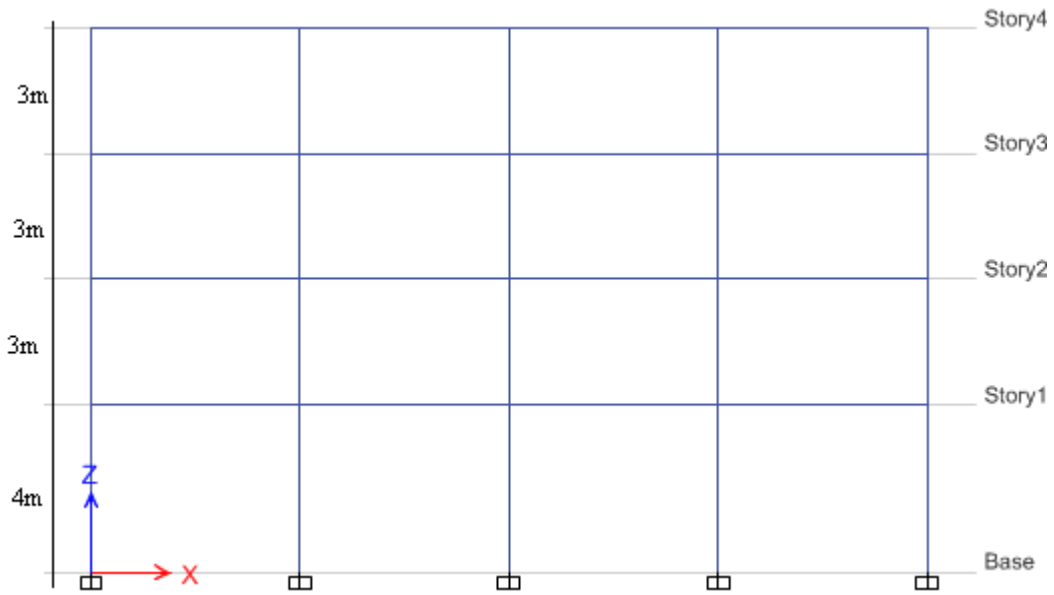

Elevation

Figure 3.7 Building configuration

4. Result and Discussion

In this chapter the result of linear and geometric nonlinear analysis is displayed and the discussion based on the result will be presented.

4.1 Flexural Members

Table 4-1 Deflection of 200 mm depth Simply Supported RC Beam length 4m

Load percentage	Load in (kN)	Deflection under the load (mm)			Difference between linear and nonlinear (%)
		Geometric Nonlinear Analysis	Linear Analysis using Staad	Linear Analysis using Scilab	
10	1.8	0.834	0.834	0.829	0.000
20	3.6	1.669	1.669	1.658	0.000
30	5.4	2.503	2.503	2.486	0.000
40	7.2	3.326	3.338	3.315	0.359
50	9	4.148	4.172	4.144	0.575
60	10.8	4.959	5.007	4.973	0.959
70	12.6	5.763	5.841	5.802	1.335
80	14.4	6.562	6.676	6.63	1.708
90	16.2	7.348	7.51	7.459	2.157
100	18	8.123	8.345	8.288	2.660

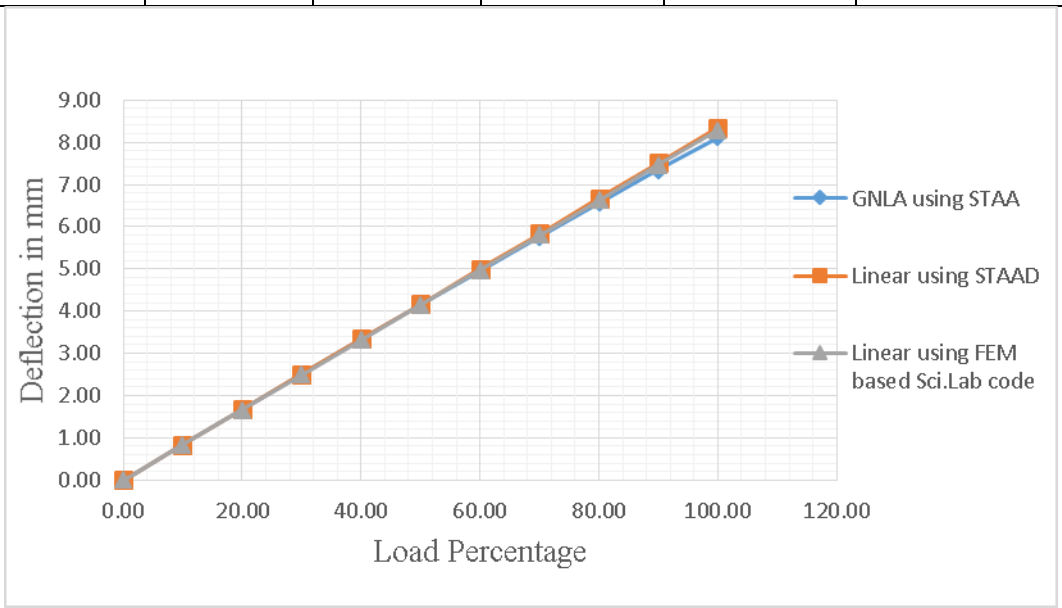

Figure 4.1 Load vs. Deflection Curve for Simply Supported Beam with depth 200 mm and 4m in length

Table 4-2 Internal effects for simple supported beam with depth 200mm and 4m in length

Internal Effects	Geometric nonlinear Analysis **(GNLA)**	Linear Analysis **(LA)**
Max Axial Force (kN)	7.499	0
Max bending moment (kNm)	17.944	18
Max Shear Force (kN)	8.973	9
Max Combined tensile Stress(N/mm^2)	10.271	10.5
Max Combined compression Stress(N/mm^2)	10.645	10.5

Load- deflection curve for simply supported beam with depth 200mm and 4m in length shows geometric nonlinear analysis result is almost similar to linear analysis and the curve is linear. In this particular flexural member the internal induced axial load due to concentrated gravity load is 7.499kN. Since the axial load small in magnitude the global stiffness matrix of member for both analysis nearly equal due to this the result from both analysis nearly equal.

Table 4-3 Deflection of 200 mm depth Simply Supported RC Beam length 6m

Load percentage	Load in (kN)	Deflection under the load (mm)			Difference between linear and nonlinear (%)
		Geometric Nonlinear Analysis	Linear Analysis using Staad	Linear Analysis using Scilab	
10	1.8	2.491	2.494	2.486	0.120
20	3.6	4.967	4.988	4.973	0.421
30	5.4	7.407	7.482	7.459	1.002
40	7.2	9.790	9.976	9.945	1.864
50	9	12.104	12.47	12.432	2.935
60	10.8	14.337	14.964	14.918	4.190
70	12.6	16.474	17.458	17.405	5.636
80	14.4	18.509	19.952	19.891	7.232
90	16.2	20.439	22.446	22.377	8.941
100	18	22.261	24.94	24.864	10.742

Table 4-4 Internal effects for simple supported beam with depth 200mm and 6m in length

Internal Effects	Geometric nonlinear Analysis **(GNLA)**	Linear Analysis **(LA)**
Max Axial Force (kN)	28.019	0
Max bending moment (kNm)	23.385	24
Max Shear Force (kN)	7.802	8
Max Combined tensile Stress(N/mm^2)	10.838	11
Max Combined compression Stress(N/mm^2)	10.239	11

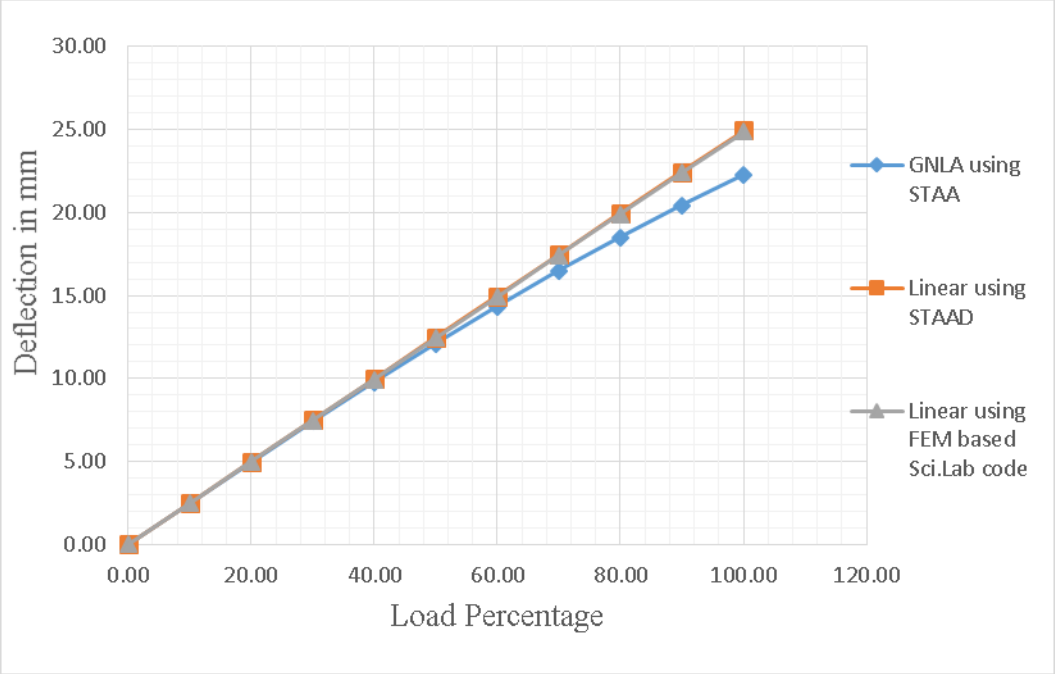

Figure 4.2 Load vs. Deflection Curve for Simply Supported Beam with depth 200 mm and 6m in length

Load – deflection curve shown in fig.4.2 shows its geometric nonlinear behavior starts at a load of forty percentage of the total load (7.2kN). Since in geometric analysis equilibrium equation of the member formulated for deformed condition of the member the stiffness matrix is also updated in each load iteration. In this flexural member the internal tensile axial load induced under geometric analysis is 28.019 kN. This tensile axial load update the stiffness matrix of the member as a result of this the flexural member becomes more stiff than that of linear analysis, in which only elastic stiffness matrix is considered by ignoring axial load effect. As a result of this the flexural

deformation under geometric analysis is lower than the corresponding flexural deformation under linear analysis with the percentage variation is 10.74. Once again the tensile and compressive stress are no more linear relationships. Since the combined tensile stress more than the compressive one with percentage variation of 6. This is due to the internal tensile axial load causes an additional tensile stress.

Table 4-5 Deflection of 200 mm depth Simply Supported RC Beam length 8m

Load percentage	Deflection under the load (mm)			Difference between linear and nonlinear (%)
	Geometric Nonlinear Analysis	Linear Analysis using Staad	Linear Analysis using Scilab	
10	3.315	3.321	3.315	0.181
20	6.591	6.642	6.630	0.768
30	9.783	9.963	9.945	1.807
40	12.854	13.283	13.260	3.230
50	15.764	16.604	16.575	5.059
60	18.489	19.926	19.890	7.212
70	21.018	23.247	23.205	9.588
80	23.343	26.568	26.520	12.139
90	25.458	29.889	29.835	14.825
100	27.374	33.209	33.150	17.571

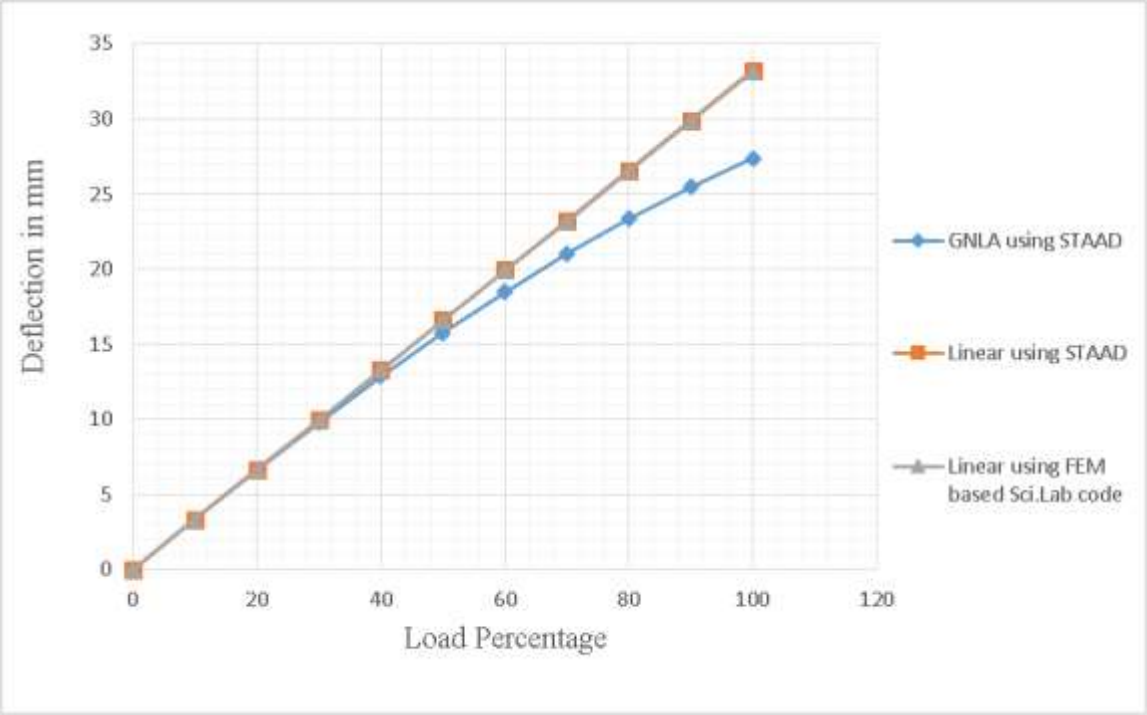

Figure 4.3 Load vs. Deflection Curve for Simply Supported Beam with depth 200 mm and 8m in length

Table 4-6 Internal effects for simple supported beam with depth 200mm and 8m in length

Internal Effects	Geometric nonlinear Analysis **(GNLA)**	Linear Analysis **(LA)**
Max Axial Force (kN)	30.685	0
Max bending moment (kNm)	17.231	18
Max Shear Force (kN)	4.314	4.5
Max Combined tensile Stress(N/mm^2)	9.256	10.5
Max Combined compression Stress(N/mm^2)	10.59	10.5

From the load –deflection curve for simply supported beam with depth 200mm and length 8m it can be observed that its geometric nonlinear behavior is starts at thirty percentage of the total load. In this member the internal tensile axial load at the early stage of load iteration is enough to make the analysis nonlinear by developing geometric stiffness matrix in addition to elastic matrix.

Table 4-7 Deflection of 300 mm depth Simply Supported RC Beam length 8m

Load percentage	Deflection under the load (mm)			Difference between linear and nonlinear (%)
	Geometric Nonlinear Analysis	Linear Analysis using Staad	Linear Analysis using Scilab	
10	1.972	1.972	1.965	0.000
20	3.941	3.944	3.929	0.076
30	5.901	5.916	5.894	0.254
40	7.847	7.889	7.858	0.532
50	9.777	9.861	9.823	0.852
60	11.689	11.833	11.787	1.217
70	13.580	13.805	13.752	1.630
80	15.441	15.777	15.716	2.130
90	17.278	17.749	17.681	2.654
100	19.082	19.721	19.645	3.240

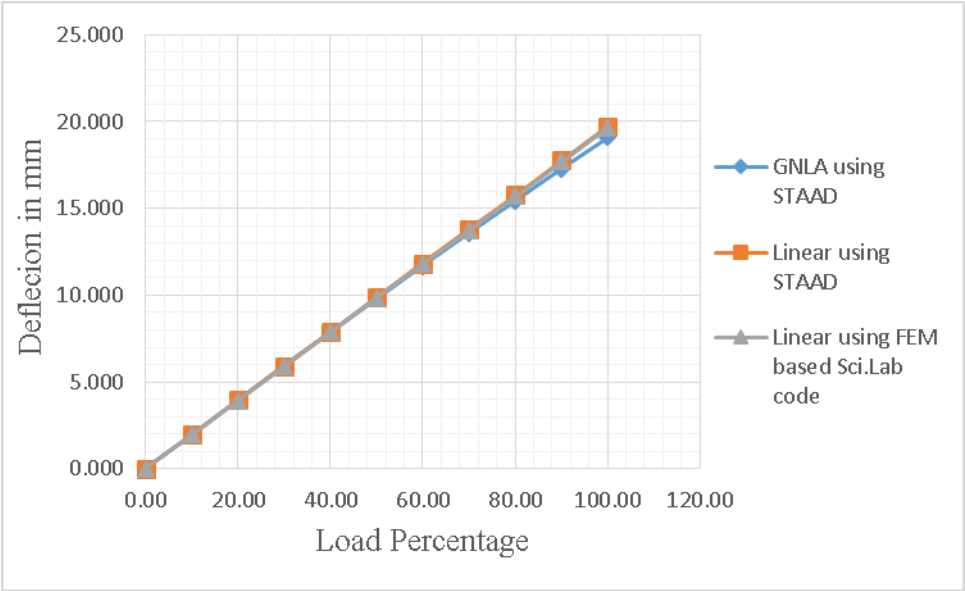

Figure 4.4 Load vs. Deflection Curve for Simply Supported Beam with depth 300 mm and 8m in length

Table 4-8 Internal Effects for simple supported beam with depth 300mm and 8m in length

Internal Effects	Geometric nonlinear Analysis **(GNLA)**	Linear Analysis **(LA)**
Max Axial Force (kN)	15.518	0
Max bending moment (kNm)	35.727	36
Max Shear Force (kN)	8.934	9
Max Combined tensile Stress(N/mm^2)	8.65	9
Max Combined compression Stress(N/mm^2)	9.168	9

From load- deflection curve shown in Fig.4.4 the nonlinear behavior starts at a load of eighty percentage (14.4kN). This tell us the geometric stiffness matrix due internal tensile axial load update the global stiffness matrix and the member starts to be stiffer than the corresponding linear analysis. As a result the flexural deformation is lower under geometric nonlinear analysis than the corresponding linear analysis.

Table 4-9 Deflection of 200 mm depth Fixed Supported RC Beam length 6m

Load percentage	Deflection under the load (mm)			Difference between linear and nonlinear
	Geometric Nonlinear Analysis	Linear Analysis using Staad	Linear Analysis using Scilab	
10	0.708	0.708	0.699	0.000
20	1.416	1.416	1.399	0.000
30	2.123	2.124	2.098	0.001
40	2.831	2.831	2.797	0.000
50	3.539	3.539	3.496	0.000
60	4.246	4.247	4.196	0.001
70	4.953	4.955	4.895	0.002
80	5.660	5.663	5.594	0.003
90	6.366	6.371	6.294	0.005
100	7.073	7.078	6.993	0.005

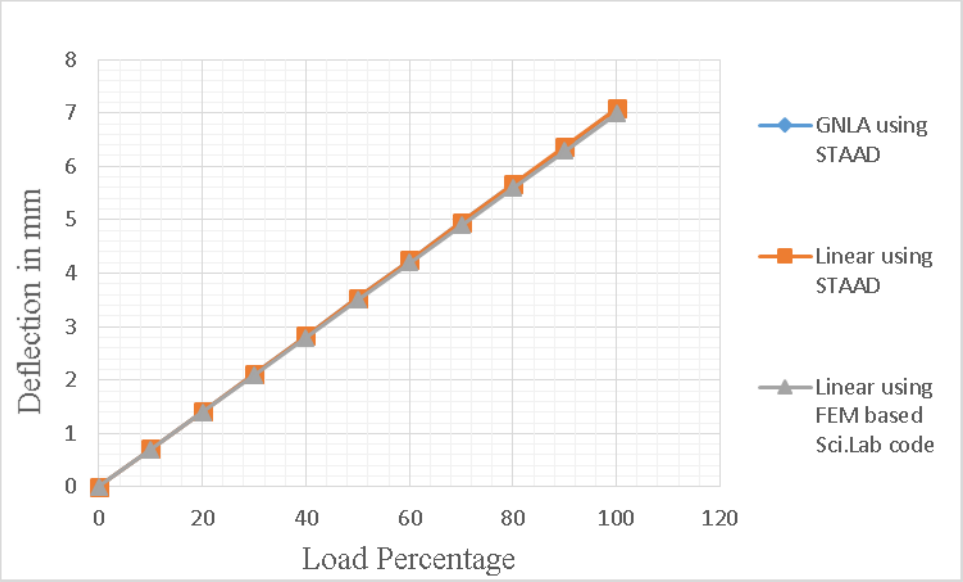

Figure 4.5 Load vs. Deflection Curve for Fixed Supported Beam with depth 200

Table 4-10 Internal reactions for Fixed supported beam with depth 200mm and 6m in length

Internal Reactions	Geometric nonlinear Analysis **(GNLA)**	Linear Analysis **(LA)**
Max Axial Force (kN)	2.415	0
Max bending moment (kNm)	13.492	13.5
Max Shear Force (kN)	8.995	9
Max Combined tensile Stress(N/mm^2)	10.059	10.125
Max Combined compression Stress(N/mm^2)	10.18	10.125

From fixed supported flexural member with depth 200mm can be observed that the curve is linear for both method of analysis. This is due to a very small internal axial load induced under geometric nonlinear analysis and the geometric stiffness matrix becomes negligible. The global stiffness matrix for both method of analysis is equal to elastic stiffness matrix of the member.

Table 4-11 Deflection of 200 mm depth Fixed Supported RC Beam subjected to external compressive axial load length 6m

Load percentage	Deflection under the load (mm)			Difference between linear and nonlinear
	Geometric Nonlinear Analysis	Linear Analysis using Staad	Linear Analysis using Scilab	
10	0.708	0.708	0.699	0.000
20	1.416	1.416	1.399	0.000
30	2.123	2.124	2.098	0.001
40	2.831	2.831	2.797	0.000
50	3.539	3.539	3.496	0.000
60	4.246	4.247	4.196	0.001
70	4.953	4.955	4.895	0.002
80	5.660	5.663	5.594	0.003
90	6.366	6.371	6.294	0.005
100	7.073	7.078	6.993	0.005

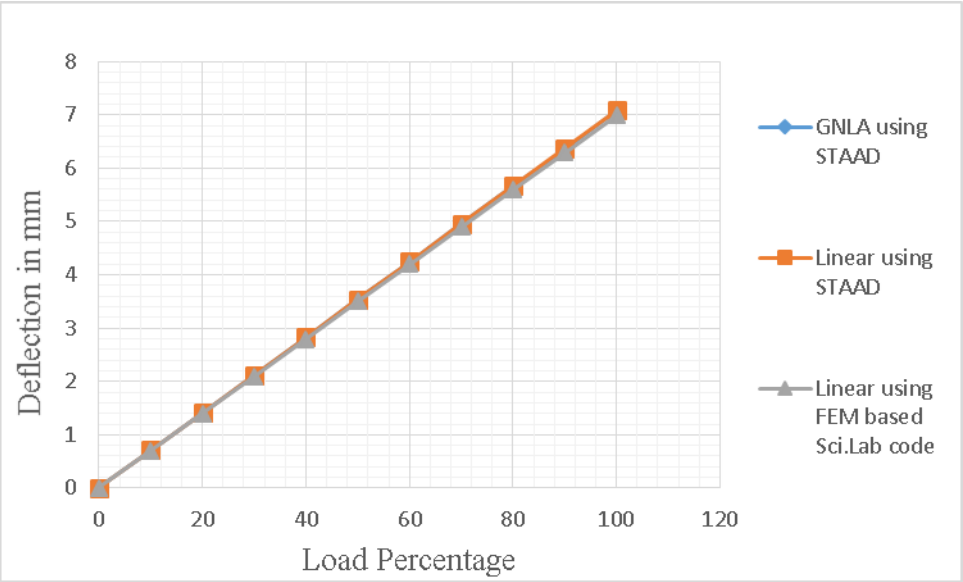

Figure 4.6 Load vs. Deflection Curve for Fixed Supported Beam with subjected to external compressive axial load depth 200

Table 4-12 Internal effects for Fixed supported beam subjected to external compressive axial load with depth 200mm and 6m in length

Internal Effects	Geometric nonlinear Analysis **(GNLA)**	Linear Analysis **(LA)**
Max Axial Force (kN)	2.415	0
Max bending moment (kNm)	13.492	13.5
Max Shear Force (kN)	8.995	9
Max Combined tensile Stress(N/mm^2)	10.059	10.125
Max Combined compression Stress(N/mm^2)	10.18	10.125

Table 4-13 Deflection of 200 mm depth simply Supported RC Beam with one end roller support and subjected to external compressive axial load length 6m

Load percentage	Deflection under the load (mm)			Difference between linear and nonlinear (%)
	Geometric Nonlinear Analysis	Linear Analysis using Staad	Linear Analysis using Scilab	
10	2.848	2.806	2.797	1.475
20	5.779	5.611	5.594	2.907
30	8.840	8.417	8.391	4.785
40	12.024	11.223	11.187	6.662
50	15.328	14.029	13.986	8.475
60	18.745	16.834	16.783	10.195
70	22.265	19.640	19.580	11.790
80	25.884	22.446	22.377	13.282
90	29.595	25.251	25.174	14.678
100	33.385	28.057	27.972	15.959

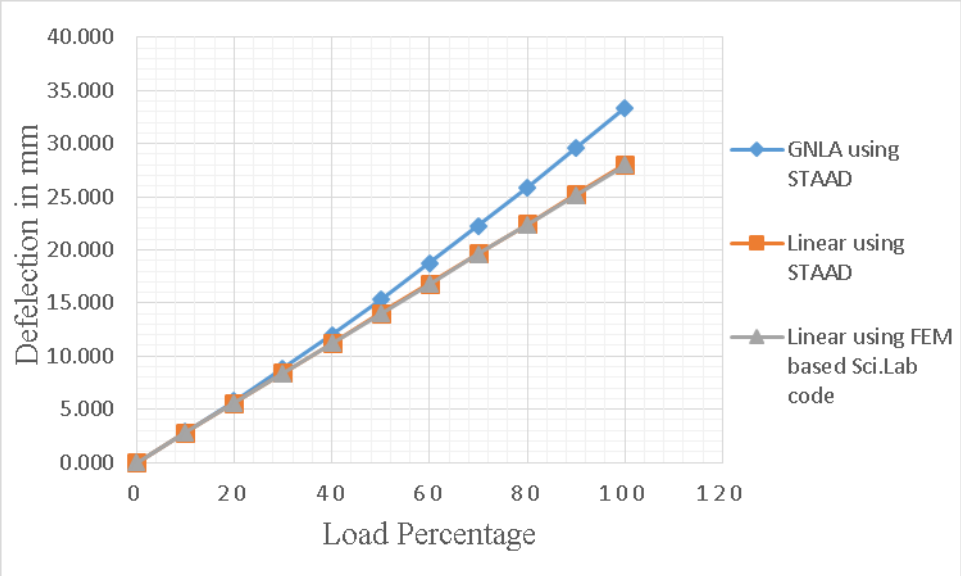

Figure 4.7 Load vs. Deflection Curve for one end roller Supported Beam with depth 200mm and 6m in length, subjected to external compressive axial load at roller end

Table 4-14 Internal effects for one end roller Supported Beam with depth 200mm and 6m in length, subjected to external compressive axial load at roller end

Internal Effects	Geometric nonlinear Analysis **(GNLA)**	Linear Analysis **(LA)**
Max Axial Force (kN)	-49.449	-50
Max bending moment (kNm)	28.44	27
Max Shear Force (kN)	9.457	9

So far the effect of internal tensile axial load that induces due to the external central point load has been discussed and it has been seen that this tensile axial load improve the stiffness matrix of flexural member results the deflection lower. Now let's apply external compressive axial load at the roller supported end of simply supported beam with depth 200mm and 6m in length. From the load- deflection curve the nonlinear behavior starts at a load of thirty percentage but here the flexural deformation under geometric nonlinear analysis is higher than the corresponding linear analysis this is due to the compressive axial load reduce the elastic stiffness matrix of the member.

Table 4-15 Deflection of 200 mm depth simply Supported RC Beam with one end roller support length 6m

Load percentage	Deflection under the load (mm)			Difference between linear and nonlinear
	Geometric Nonlinear Analysis	Linear Analysis using Staad	Linear Analysis using Scilab	
10	2.806	2.806	2.797	0.014
20	5.611	5.611	5.594	0.056
30	8.418	8.417	8.391	0.141
40	11.227	11.223	11.187	0.267
50	14.036	14.029	13.986	0.433
60	16.847	16.834	16.783	0.637
70	19.659	19.640	19.580	0.875
80	22.472	22.446	22.377	1.146
90	25.287	25.251	25.174	1.448
100	28.103	28.057	27.972	1.776

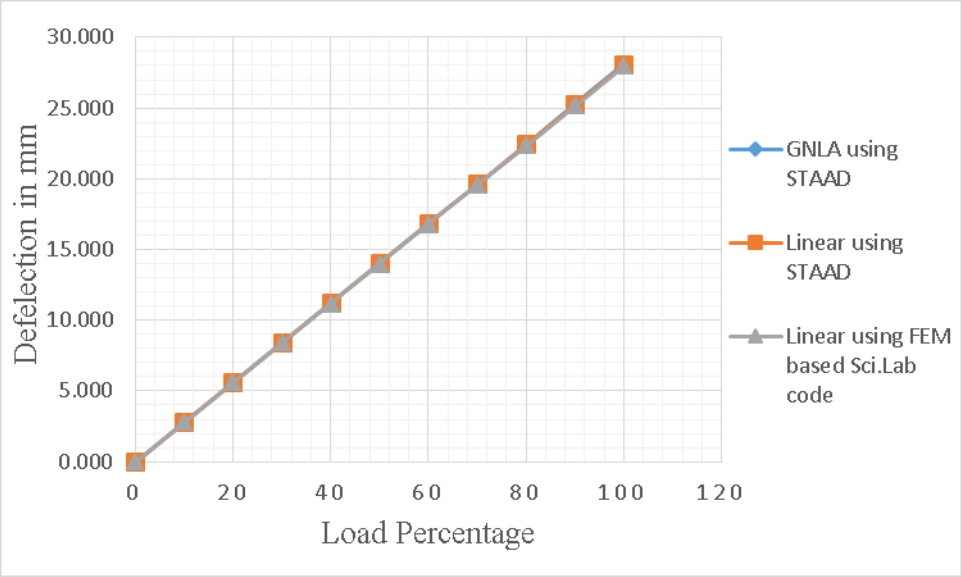

Figure 4.8 Load vs. Deflection Curve for one end roller Supported Beam with depth 200mm and 6m in length

Table 4-16 Internal effects for one end roller Supported Beam with depth 200mm and 6m in length

Internal Effects	Geometric nonlinear Analysis **(GNLA)**	Linear Analysis **(LA)**
Max Axial Force (kN)	0.455	0
Max bending moment (kNm)	26.988	27
Max Shear Force (kN)	8.996	9

The result obtained from geometric nonlinear analysis for simply supported beam with one end roller support, which is subjected to only gravity load, is almost linear. Since there is an axial deformation under geometric analysis the stress in the member is reduce result in very small tensile axial load is induced.

Table 4-17 Axial Deflection of 200 mm depth simply Supported RC Beam with one end roller support and subjected to external compressive axial load length 6m

Load percentage	Axial Deflection at Node 1(at appoint of axial load is applied) (mm)			Difference between linear and nonlinear
	Geometric Nonlinear Analysis	Linear Analysis using Staad	Linear Analysis using Scilab	
10	0.037	0.035	0.035	0.002
20	0.08	0.069	0.069	0.011
30	0.128	0.104	0.104	0.024
40	0.182	0.138	0.138	0.044
50	0.242	0.173	0.173	0.069
60	0.309	0.207	0.207	0.102
70	0.382	0.242	0.242	0.14
80	0.461	0.276	0.276	0.185
90	0.548	0.311	0.311	0.237
100	0.641	0.345	0.345	0.296

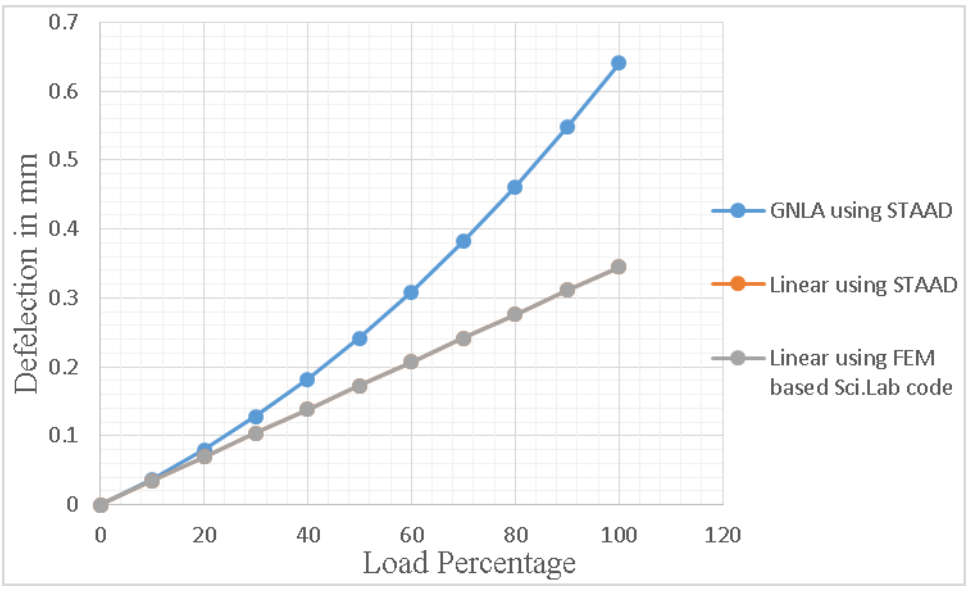

Figure4.9 Load vs. Deflection Curve for one end roller Supported Beam with depth 200mm and 6m in length, subjected to external compressive axial load at roller end

4.2 Four Story RC building Frame

Analysis is done using STAAD Pro for both linear and geometric nonlinear case and ETABS for linear case. In the first part of the analysis only the lateral forces that is obtained from equivalent static analysis based on EBCS EN 1998(part 8) has been considered.

The lateral forces on building frame are obtained by seismic equivalent static analysis is given in Fig.4.10 in the second part of the analysis both seismic equivalent lateral forces and gravity load are considered as shown in Fig 4.12.

4.2. 1 Four Story RC building Frame under Lateral Load

After the frame is analysed the load- deflection curve for flexural member at second story between axis A and B is shown in Fig 4.11. From the curve the nonlinear behavior starts at a load of thirty percentage. Since a compressive axial load is induced in flexural member due to external lateral force the global stiffness matrix will be reduced and this result the deflection is more under geometric nonlinear analysis than the corresponding linear analysis. This is based on the fact that the geometric stiffness matrix due to compressive axial load is negative and it reduce the elastic stiffness matrix of a member when the global stiffness matrix is calculated.

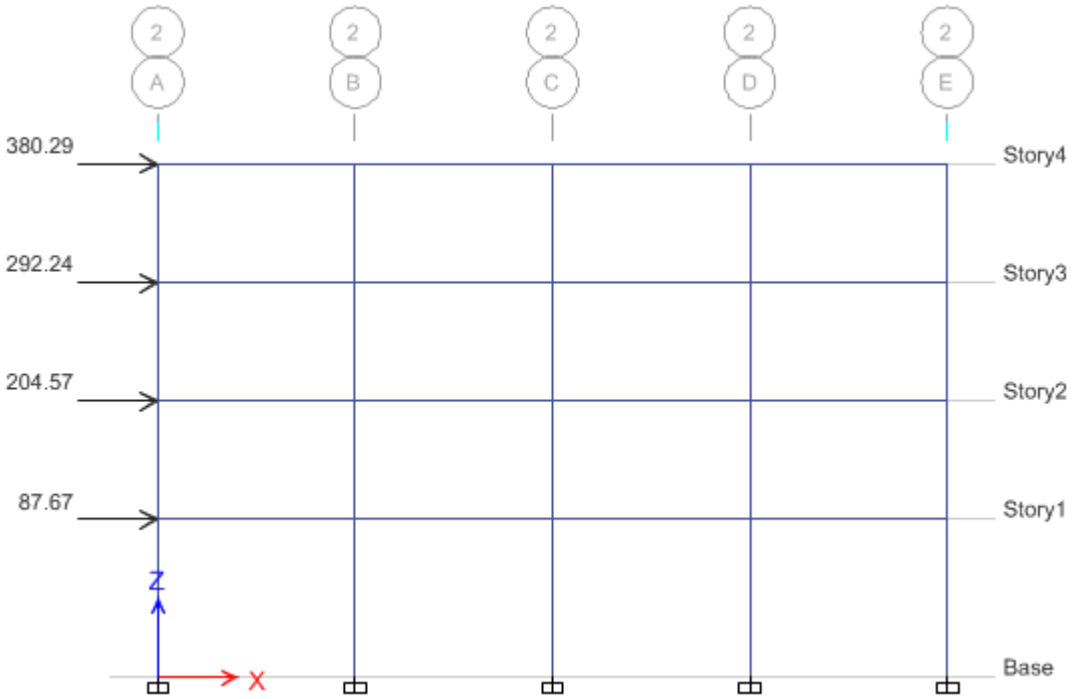

Figure 4.10 Lateral forces on building frame by equivalent static method

Table 4-18 Deflection of flexural member at Second Story Between axis A and B

Load percentage	Deflection under the load (mm)			Difference between linear and nonlinear
	Geometric Nonlinear Analysis	Linear Analysis using Staad	Linear Analysis using ETABS	
10	1.119	1.099	1.199	0.020
20	2.276	2.198	2.298	0.078
30	3.473	3.297	3.397	0.176
40	4.711	4.396	4.496	0.315
50	5.989	5.495	5.595	0.494
60	7.307	6.594	6.694	0.713
70	8.665	7.693	7.793	0.972
80	10.062	8.792	8.892	1.270
90	11.498	9.891	9.991	1.607
100	12.973	10.994	11.094	1.979

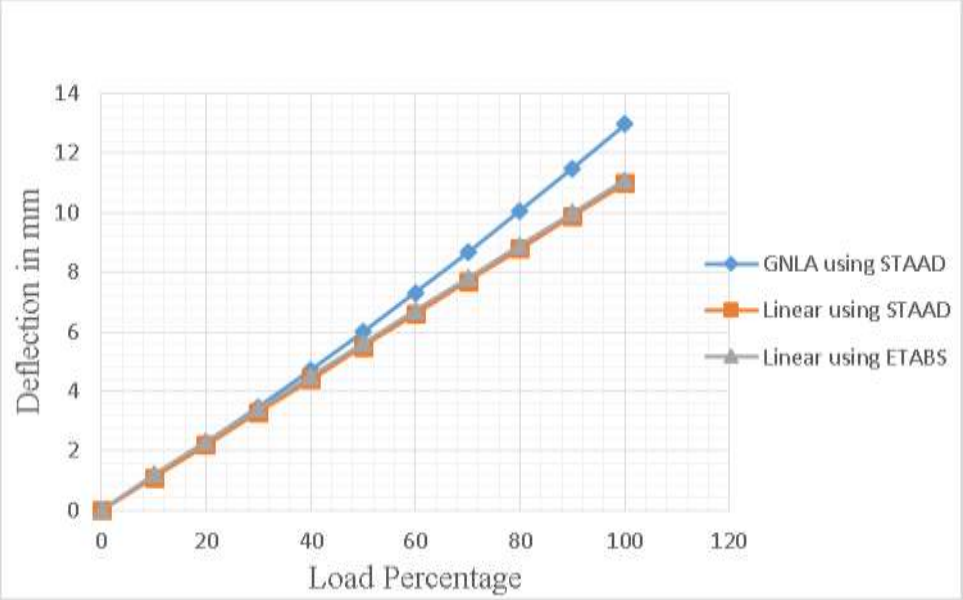

Figure 4.11 Load – Deflection curve of Second Story Flexural Member between Axis A & B

4.2.2 Four Story RC building Frame under Lateral and Gravity Load

Now the frame is analysed for both load cases. From the load- deflection curve shown in Fig 4.13. The nonlinear behavior o starts at a load of twenty percentage. Once again due to compressive axial load the global stiffness matrix become lower than the elastic one under geometric nonlinear analysis and result in higher deflection.

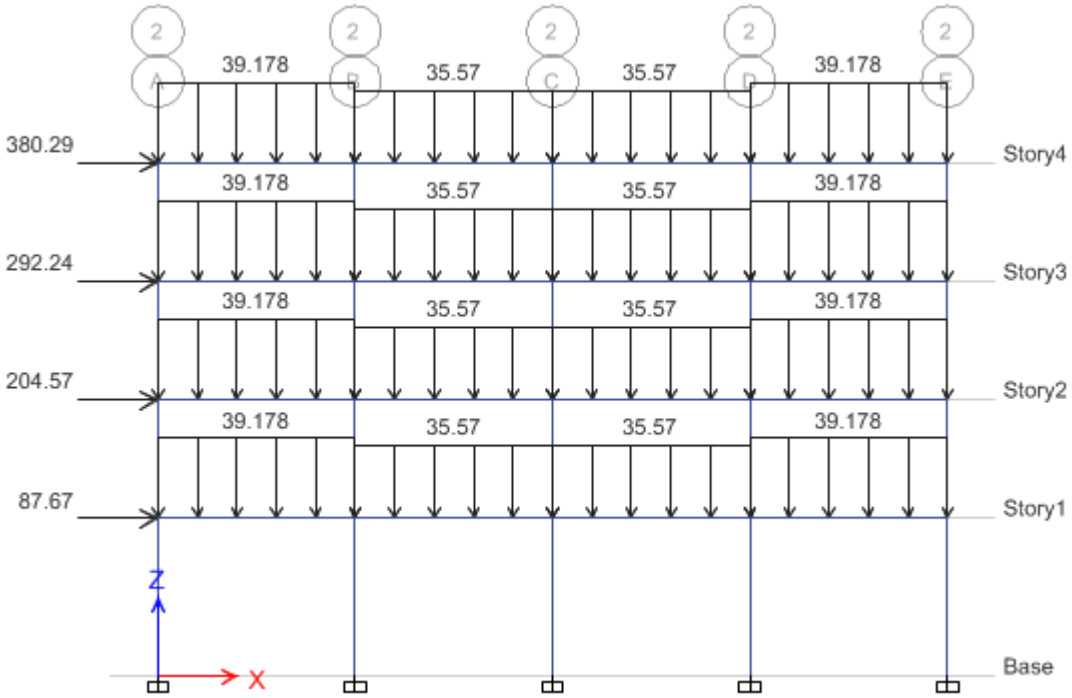

Figure 4.12 Lateral forces and Gravity on building frame

Table 4-19 Deflection of flexural member at Second Story Between axis A and B

Load percentage	Deflection under the load (mm)			Difference between linear and nonlinear
	Geometric Nonlinear Analysis	Linear Analysis using Staad	Linear Analysis using ETABS	
10	1.604	1.578	1.538	0.026
20	3.261	3.156	3.116	0.105
30	4.973	4.734	4.694	0.239
40	6.743	6.312	6.272	0.431
50	8.572	7.890	7.850	0.682
60	10.462	9.468	9.428	0.994
70	12.421	11.046	11.006	1.375
80	14.438	12.624	12.584	1.814
90	16.527	14.202	14.162	2.325
100	18.680	15.776	15.736	2.904

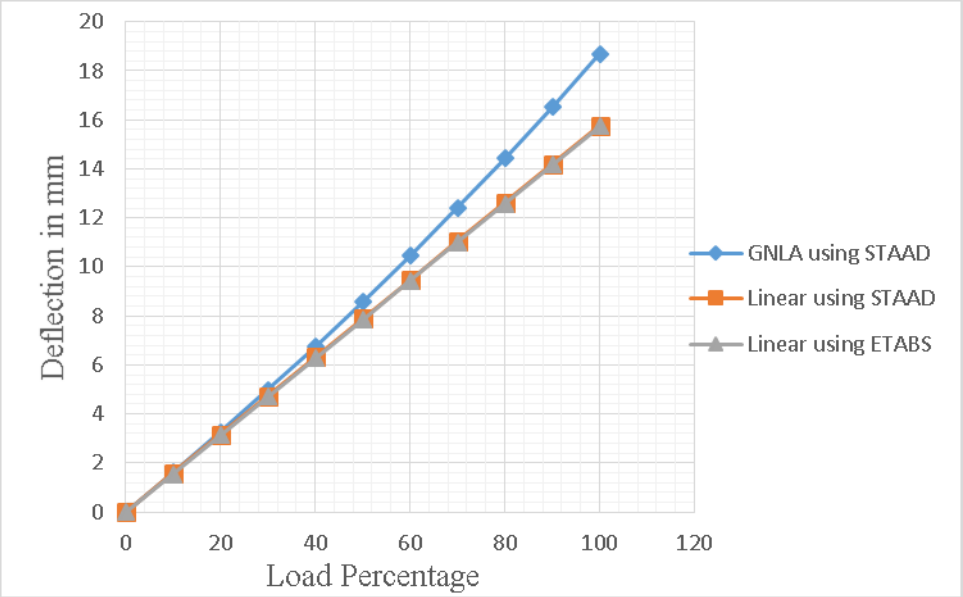

Figure 4.13 Load – Deflection curve of Second Story Flexural Member between Axis A & B

For the flexural member at the fourth story between axis A and B it is observed similar scenario in fact its nonlinear behavior starts at early load percentage than the flexural member at the second story this is due the fact that the compressive axial load at the forth story member is more than the second story member. Therefore the corresponding percentage variation of flexural deformation under geometric nonlinear analysis and linear analysis is 25.22.

Table 4-20 Deflection of flexural member at Fourth Story Between axis A and B

Load percentage	Deflection under the load (mm)			Difference between linear and nonlinear
	Geometric Nonlinear Analysis	Linear Analysis using Staad	Linear Analysis using ETABS	
10	1.127	1.093	1.043	0.034
20	2.320	2.186	2.136	0.134
30	3.591	3.279	3.229	0.312
40	4.934	4.372	4.322	0.562
50	6.354	5.465	5.415	0.889
60	7.853	6.558	6.508	1.295
70	9.437	7.651	7.601	1.786
80	11.103	8.744	8.694	2.359
90	12.858	9.837	9.787	3.021
100	14.702	10.930	10.880	3.772

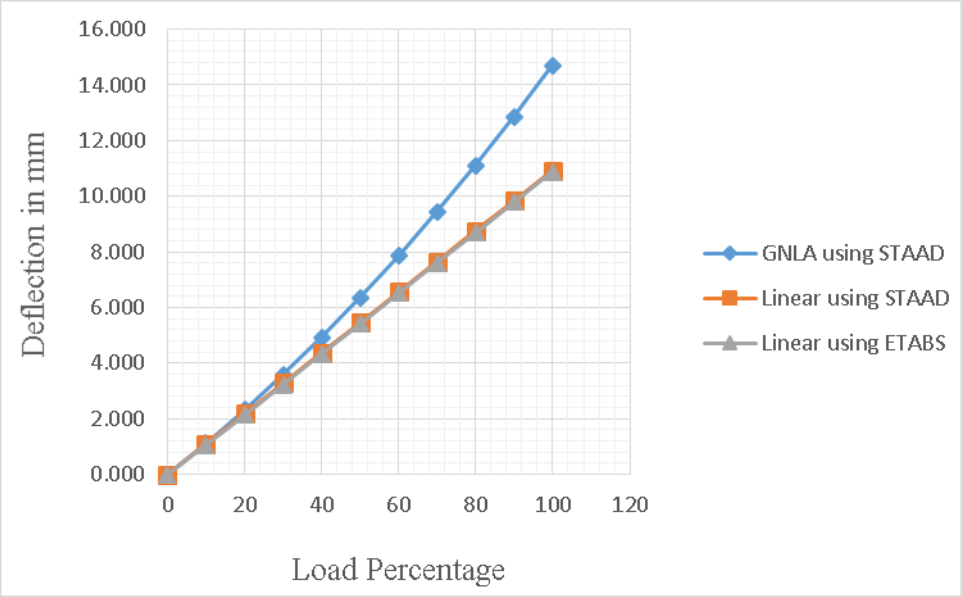

Figure 4.14 Load – Deflection curve of Fourth Story Flexural Member between Axis A & B

4.3 Comparison

Table 4-21 Percentage Variation of Linear and Geometric Nonlinear Deflection of Beam with Different Span Length

Load percentage	Percentage variation of linear and Geometric nonlinear(L=4m)	Percentage variation of linear and Geometric nonlinear(L=6m)	Percentage variation of linear and Geometric nonlinear(L=8m)
10	0.00	0.120	0.181
20	0.00	0.421	0.768
30	0.00	1.002	1.807
40	0.359	1.864	3.230
50	0.575	2.935	5.059
60	0.959	4.190	7.212
70	1.335	5.636	9.588
80	1.708	7.232	12.139
90	2.157	8.941	14.825
100	2.660	10.742	17.571

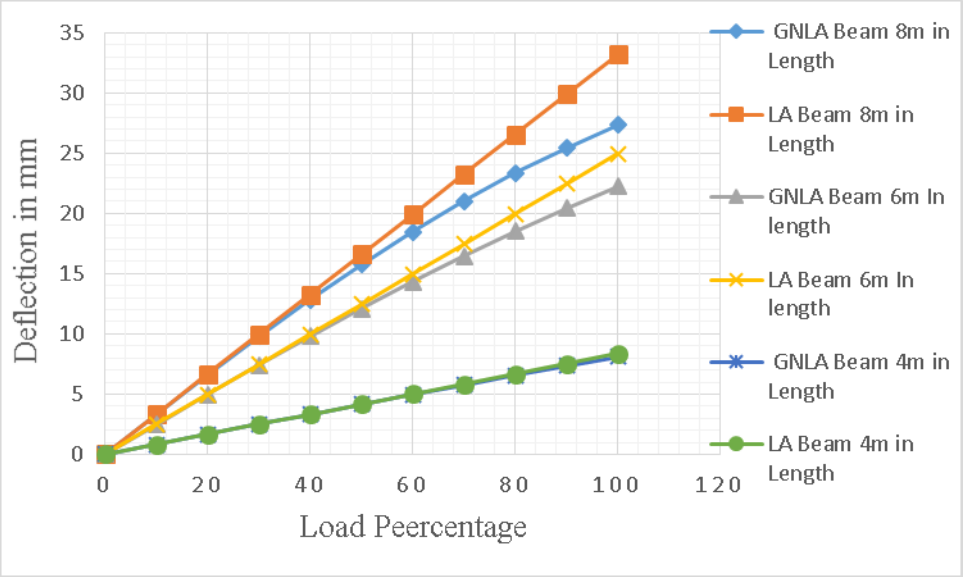

Figure 4.15 Load Deflection Curve of Beam with Different Span Length

Load – deflection curve shown in Fig.4.15 shows that the axial effect under geometric nonlinear analysis increase as the length of the flexural member increases. The percentage difference between linear and geometric nonlinear deflection is more in case of simply supported beam with longer span length as shown in table 4.21. This is due to the fact that the induced tensile axial load is increases as span length the flexural member increases.

Table 4-22 Percentage Variation of Linear and Geometric Nonlinear Deflection of Beams with Different depth

Load percentage	Percentage variation of linear and Geometric nonlinear (H=200mm)	Percentage variation of linear and Geometric nonlinear (H=300mm)
10	0.181	0.000
20	0.768	0.076
30	1.807	0.254
40	3.230	0.532
50	5.059	0.852
60	7.212	1.217
70	9.588	1.630
80	12.139	2.130
90	14.825	2.654
100	17.571	3.240

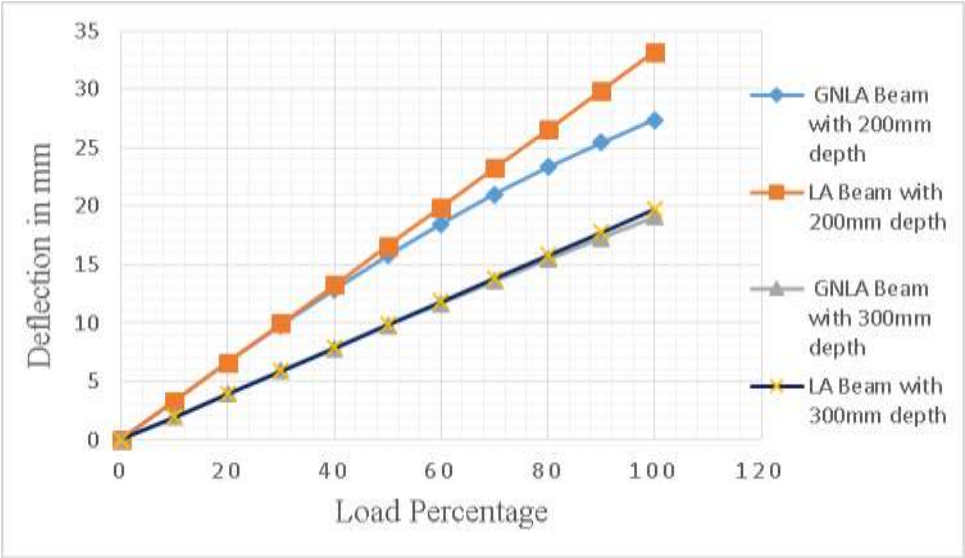

Figure 4.16 Load Deflection Curve of Beam with Different Depth

In full load condition the percentage variation of linear and geometric nonlinear flexural deformation is 17.571 for flexural member having 200mm depth while it is only 3.240 for beam with 300mm depth. The tensile axial; load induced in 200mm beam is 30.685kN while is 15.518kN in beam 300mm in depth under geometric nonlinear analysis this makes big difference in deflection. Hence the depth of beam affects the behavior of beams significantly.

Table 4-23 Percentage Variation of Linear and Geometric Nonlinear Deflection of Beam with Different End Conditions

Load percentage	Percentage variation of linear and Geometric nonlinear **Simply supported**	Percentage variation of linear and Geometric nonlinear **Fixed Supported**
10	0.120	0.000
20	0.421	0.000
30	1.002	0.000
40	1.864	0.000
50	2.935	0.000
60	4.190	0.001
70	5.636	0.002
80	7.232	0.003
90	8.941	0.005
100	10.742	0.005

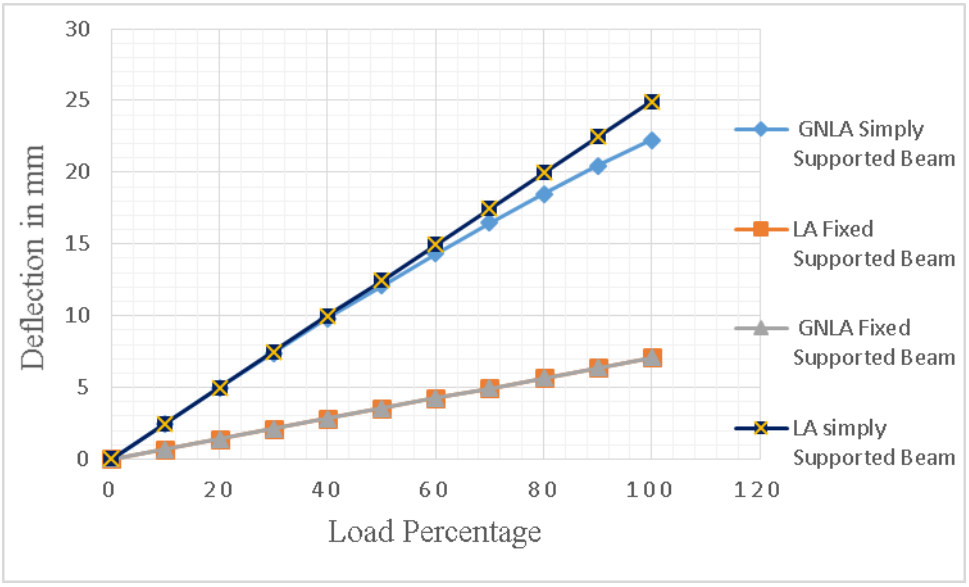

Figure 4.17 Load Deflection Curve of Beam with Different End Conditions

The difference between linear and geometric nonlinear deflection is more in case of simply supported beam with depth 200mm and 6m in length. The tensile axial load in simply supported beam is 28.019kN while it is only 2.415kN in fixed supported beam this make the corresponding percentage variation of linear and geometric nonlinear deflection is more in simple supported beam than the fixed one as shown in table 10.742.

5 Conclusions and Recommendations

In this thesis the linear and geometric nonlinear flexural deformation of reinforced concrete members subjected to central point load and with and without external compressive axial load was carried out to investigate the effect of axial load. Four story RC residential building is analysed and the flexural deformation behavior of selected flexural member was studied for the illustration of linear and geometric nonlinear effect of axial load in actual building frame. The studies on software and theoretical results associated with them lead to the following conclusion and recommendations.

5.1 Conclusions

- Linear analysis of flexural members ignore the effect of axial load in flexural deformation this result in uneconomical design since it over estimates the flexural deformation under gravity load.
- Support conditions affect variation of flexural deflection between linear and geometric nonlinear analysis considerably. For fixed end flexural members the variation between linear and geometric nonlinear deflection is negligible but same flexural member with simply supported condition was giving variation in deflection up to 17.57 percent.
- At initial stage of loading the effect of axial load is negligible as a result the flexural deflection behavior of linear and geometric nonlinear analysis is linear. While it becomes nonlinear with increasing the load value.
- Geometric nonlinearity is not induced in the higher depth beam when the load intensity is small and it is induced in the higher depth beam when the big load intensity goes on increasing.
- Geometric nonlinearity is induced in the beam because of its lesser depth. It is produced more in the lesser depth beam, when load is increased.
- As the deforming of middle plane (Neutral axis) starts, the stiffness of structure increases (axial stiffness is added with bending stiffness).Thus the beam becomes stiffer progressively. It is a positive aspect of geometric nonlinearity.

5.2 Recommendations

- The flexural members ‘strength significantly modified in the present of tension or compression axial load. The tensile axial load increase the strength of the flexural members by modifying its stiffness while the compressive axial load reduce its strength under geometric nonlinear analysis.
- The effect of axial load under geometric nonlinear analysis is very significant for sections with lesser depth, it is better to analyses RC building which contains such kinds of members using geometric nonlinear analysis.
- RC building which is located in seismic zone is subjected lateral load which induce compression axial load on flexural members and this compression axial load reduce its stiffness so the flexural deflection become higher than the corresponding linear analysis. Therefore it is better to analysis such building using geometric nonlinear analysis.
- To be safe and economical it is better to study the real behavior of our structure. The real behavior of the structure is nonlinear in its nature. Therefore it is advisable to analysis using nonlinear analysis and compare their result with the linear analysis and then design the structures based on the governed method of analysis.

Reference

[1] D. D. C. W. D. H. Nilson, Design of Concrete Structures, New York: Mc Graw-Hill companies. Inc., 2010.

[2] S. Mr. Kashinath N. Borse, "Geometric Linear And Nonlinear Analysis Of Beam," vol. Vol. 2, no. 7, 2013.

[3] K. K. R. M. a. U. K. Dewangan, "Comparative Study of Linear and Geometric Nonlinear Load-Deflection Behavior of Flexural Steel Members," vol. 9(18), no. 0974-6846, 2016.

[4] V. E. Saouma, Finite Element II Solid mechanics, Boulder: University of Colorado, Spring, 2001.

[5] J. S. Przemieniecki, THEORY OF MATRIX STRUCTURAL ANALYSIS, New York: DOVER PUBLICATIONS, INC., 1968.

[6] R. D. Cook, Finite Element Modeling for Stress Analysis, Canada: John wileyy & Sons.Inc, 1995.

[7] SS.Bhavikatti, Finite element Analysis, New Delhi: New Age International(P) Ltd., Publishers, 2005.

[8] C. A. Felippa, "http://www.colorado.edu/engineering/cas/courses.d/NFEM.d/," University of Colorado at Boulder, Department of Aerospace Engineering Science, 28 April 2016. [Online]. [Accessed 03 March 2017].

[9] A. A. D. A. E. p. D. C. E. Sousa, "Aspects on Nonlinear Geometric and Material Analysis of Three-Dimensional Framed Structures," Faculdade de Engenharia, Universidade, Porto, 2009.

[10] Ş. D. A. ,. M. Ş. T. Kocatürk, "Large Deflection Static Analysis of a Cantilever

Beam Subjected to a Point Load," vol. 2, no. 4(2010)1-13, 2010.

[11] U. K.K.Riyas Moideen, ""Comparative Study of Linear Geometric nonlinear Load-Deflection Behaviour of Flexural Steel Member"," vol. 19(18), no. 0974-5645, 2016.

[12] F. V. H. T. P. S. Wong, "VECTOR2 & FORMWORKS USER'S MANUAL," Auigest 2002.

[13] Y.-F. Wu, "Theorems for Flexural Design of RC Members," no. 0733-9445, 2015.

[14] M. S. a. M. K. S. M. Shantaram G. Ekhande, "Stability Functions for three - Dimensional Beam- Columns," vol. 115, no. 0733-9445/89/0O02-0467/, 1989.

[15] A. T. a. A. Alarcón, "Automated design of optimum longitudinal reinforcement for flexural and axial loading," vol. 10, no. 2 (2012) 149-171, January 16, 2012.

[16] R. Sezer, "The geometrical nonlinear analysis of the prismatic plane frames with the stiffness matrice method," vol. 5(22), no. 992-2248, 2010.

[17] G. S. a. S. Banu, "Buckling load OF a Beam-Column for Different End Conditions Using Multi-Segment Integration Technique," vol. 2, no. 1819-6608, 2006 - 2007.

[18] S.S.Bhavikatti, Finite Element Analysis, New Delhi: New Age International (P) Ltd, 2005.

[19] ASCE-ACI Committee 445, "Recent Approaches to Shear Design of Structural Concrete," *American Society of Civil Engineers*, December 1998.

[20] Transportation Reasearch Board Executive Commitee , "Simplified Shear Design of Structural Concrete Members," *NCHRP*, vol. NCHRP REPORT 549, 2005.

[21] M. P. Collins, E. C. Bentz, E. G. Sherwood and L. Xie, "AN ADEQUATE THEORY FOR THE SHEAR STRENGTH OF REINFORCED CONCRETE STRUCTURES," 2007.

[22] ACI Commitee 318, "Building Code Requirements for Structural Concrete (ACI 318-14) AND Commentary on Building Code Requirements for Structural Concrete (ACI 318R-14)," 2014.

[23] A. H. Nilson, D. Darwin and W. C. Dolan, Design of Concrete Structures, 14th edition ed., New York: Mc Graw Hill Companies, 2010.

[24] C. E. Bentz, F. J. Vecchio and M. P. Collins, "Simplified Modified Compression Field Theory for Calculating Shear Strength of Reinforced Concrete Elements," vol. ACI Structural Journal, no. July-August, 2006.

[25] K. J. Weight and J. G. Macgregor, Reinforced Concrete Mechanics & Design, 6th edition ed., New Jersey: Pearson Education, 2012.

[26] M. Peter, "Truss Models in Detailing," 1985.

[27] M. Ghoneim and M. EL-Mihilmy, Design of Reinforced Concrete Structures, 2nd edition ed., Cairo University, 2008.

[28] M. Zakaria, T. Ueda, Z. Wu and L. Meng, "Experimental Investigation on Shear Cracking Behavior in Reinforced Concrete Beams with Shear Reinforcement," 2009.

[29] M. Aruna, "Shear Behavior of Concrete Beams Reinforced with High Performance Steel Shear Reinforcement," 2008.

Appendix A Finite Element method Based Scilab.code

```
// 3 noded 20X20 Simply supported beam L=4m//
E=21.7185
I=200^4/12
L=2000
P=-18
K=(E*I/L^3)*[4*L^2,-6*L,2*L^2,0;
-6*L,24,0,6*L;
2*L^2,0,8*L^2,2*L^2;
0,6*L,2*L^2,4*L^2]
KK=inv(K)
f=[0;P;0;0]
d=KK*f

// 3 noded 20X20 Simply supported beam L=6m//
E=21.7185
I=200^4/12
L=3000
P=-16
K=(E*I/L^3)*[4*L^2,-6*L,2*L^2,0;
-6*L,24,0,6*L;
2*L^2,0,8*L^2,2*L^2;
0,6*L,2*L^2,4*L^2]
KK=inv(K)
f=[0;P;0;0]
d=KK*f


// 3 noded 20X20 Simply supported beam L=8m//
E=21.7185
I=200^4/12
L=4000
P=-9
K=(E*I/L^3)*[4*L^2,-6*L,2*L^2,0;
-6*L,24,0,6*L;
2*L^2,0,8*L^2,2*L^2;
0,6*L,2*L^2,4*L^2]
KK=inv(K)
f=[0;P;0;0]
d=KK*f



// 3 noded 20X30 Simply supported beam L=8m//
E=21.7185
I=200*300^3/12
L=4000
P=-18
K=(E*I/L^3)*[4*L^2,-6*L,2*L^2,0;
-6*L,24,0,6*L;
2*L^2,0,8*L^2,2*L^2;
0,6*L,2*L^2,4*L^2]
KK=inv(K)
f=[0;P;0;0]
d=KK*f


// 3 noded 20X20 Fixed supported beam L=8m//
E=21.7185
I=200^4/12
L=4000
P=-11
Keff=(E*I/L^3)*[24,0,;0,8*L^2]
```

```
KK=inv(Keff)
f=[P;0]
d=KK*f

// 3 noded 20X20 Simply supported beam L=6m one end with roller support//
E=21.7185
I=200^4/12
A=200*200
L=3000
P=-18
Pa=0
K=(E*I/L^3)*[A*L^2/I,0,-A*L^2/I,0,0,0;
0,4*L^2,0,-6*L,0,0;
-A*L^2/I,0,2*(A*L^2/I),0,0,0;
0,-6*L,0,24,6*L,6*L;
0,2*L^2,0,0,4*L^2,2*L^2;
0,0,0,6*L,2*L^2,4*L^2]
KK=inv(K)
f=[Pa;0;0;P;0;0]
d=KK*f

// 3 noded 20X20 Simply supported beam L=6m one end with roller support//
// which is subjected to axial load inaddition to gravity load//
E=21.7185
I=200^4/12
A=200*200
L=3000
P=-18
Pa=50
Keff=(E*I/L^3)*[A*L^2/I,0,-A*L^2/I,0,0,0;
0,4*L^2,0,-6*L,0,0;
-A*L^2/I,0,2*(A*L^2/I),0,0,0;
0,-6*L,0,24,6*L,6*L;
0,2*L^2,0,0,4*L^2,2*L^2;
0,0,0,6*L,2*L^2,4*L^2]
KK=inv(Keff)
f=[Pa;0;0;P;0;0]
d=KK*f
```